ASHESI

ASHESI UNIVERSITY

THE ROLE OF MECHANICAL STIMULI ON BACTERIA GROWTH

APPLIED CAPSTONE PROJECT

B.Sc. Mechanical Engineering

Nana Oye Ndaase Djan

2019

ASHESI UNIVERSITY

THE ROLE OF MECHANICAL STIMULI ON BACTERIA GROWTH

APPLIED CAPSTONE PROJECT

Capstone Project submitted to the Department of Engineering, Ashesi University in partial fulfilment of the requirements for the award of Bachelor of Science degree in Mechanical Engineering.

Nana Oye Ndaase Djan

2019

Declaration

I hereby declare that this capstone is the result of my own original work and that no part of it has been presented for another degree in this university or elsewhere.

Candidate's Signature:

……

Candidate's Name:

……

Date:

……

I hereby declare that preparation and presentation of this capstone were supervised in accordance with the guidelines on supervision of capstone laid down by Ashesi University.

Supervisor's Signature:

……

Supervisor's Name:

……

Date:

……

Acknowledgements

First and foremost, I am grateful to God for bringing me this far. I am also very grateful to my supervisor, Dr. Elena Rosca for her dedication and great contribution during the supervision of this project.

Special appreciation and thanks to my family for simply being there for me. I also thank the entire engineering faculty for their immense support in ensuring that my journey in Ashesi culminated in this wonderful thesis.

Abstract

Synthetic biology is the engineering of biology; it is the evaluation and design of biological systems in a rational and systematic manner. It blurs the lines between various science and engineering disciplines due its numerous applications, with one of the most significant being the use of biosensors in environmental remediation. Biosensors substitute engineered micro-organisms as traditional sensors and transducers. In recent years, the use of *E. coli* as the primary micro-organism in biosensors has gained popularity simply because of the ease of use, stability, etc. However, the effect of the environment on the biosensor has largely been ignored, especially the effect of mechanical stimuli, such as viscosity of the fluid medium, direction and speed of motion, etc. The main output of this project was an incubator containing a robotic platform that varied the direction of motion. The temperature in the incubator is controlled by proportional controller using the measured temperature as feedback to tune the system's response. A simple mathematical model (based on the traditional logistic curve) was formulated with an added term that incorporated the effect of the movement of the robotic platform in the form of shear stress. The model proved that mechanical stimuli can affect generation time of *E.coli* by varying one of the model's parameters. The next step therefore is to fit data to the model to determine the value of the parameter varied.

Table of Contents

List of Abbreviations

A/D – Analog to Digital

D/A – Digital to Analog

DOF's – Degrees of Freedom

E.coli – *Escherichia Coli*

FRET – Forster Resonance Energy Transfer

iGEM – International Genetically Engineered Machine

LCD – Liquid Crystal Display

PLA – Polylactic acid

PD – Proportional, Derivative

PI – Proportional, Integral

PID – Proportional, Integral, Derivative

POCD – Point of Care Device

List of Figures

List of Tables

Chapter 1: Introduction

1.1.Background Information

Biosensors are devices that convert biological responses into a quantifiable response, usually any response that can be converted to an electrical or optical signal for easy processing and data storage [1]. Oftentimes, biosensors can be classified into three main categories based on their biorecognition principles: the biocatalytic group usually including enzymes, the bio-affinity group, which includes antibodies and nucleic acids and the microbe-based group, whose functionality is based on changes in specific features of a microorganism [2]. The common element that runs through all biosensors is a highly sensitive biological component that has been engineered to respond in a highly selective manner to a target analyte [1].

The microbe-based group has gained popularity in the field of synthetic biology, due to their intrinsically modular makeup [3]. A modular design approach simply breaks up a system into smaller parts that can be studied independently and even used in other systems. One of the main sub-divisions of the microbe-based biosensor, is, without question, the micro-organism that responds to changes in a target analyte. Bacteria is the most commonly used micro-organism in whole cell biosensors due to its fast growth rate, easy manipulation, relatively better stability and variety of species to choose from, especially in the context of synthetic biology [3].

Unfortunately, until about a decade ago, only the biological stimuli that impacted the growth and response of bacteria has been studied to a large extent [4]. The effect of other stimuli, such as mechanical stimuli have not been studied into much detail [4].

For instance, in 2017, a group of engineers from Ashesi University attempted to tackle the issue of gold mining, utilizing a biosensor as part of their project design. This was in fulfillment of the deliverables of their iGEM project. To create a lasting solution that is sustainable and environmentally friendly, they designed and partially implemented a genetically engineered device capable of detecting, quantifying and liberating gold from ore. However, challenges with procuring essential equipment such as incubators seemed to hinder the growth rate of the bacteria as well protein production in the bacteria as the conditions necessary for optimal bacterial growth were not fulfilled. Thus, understanding how the changes in the growth environment affects the organism would have been helpful to their research and probably to many other researchers as well.

1.2.Project Aims and Objectives

The main aim of this project is therefore to investigate the effect of mechanical stimuli on bacterial growth. In line with this, the specific objectives of this project are as follows:

- To investigate the effect that mechanical stimuli have on bacteria growth using a mathematical model.
- To fabricate an incubator that can provide the optimal mechanical and temperature control for bacteria growth.

1.3.Expected Outcomes of Project

It is expected that at the completion of this project the result will be a robust understanding on how bacteria growth responds to differences in the direction of motion applied as well as the speed of motion giving a comprehensive understanding of how the manipulation of these factors can be used in the design of future biosensors.

1.4.Problem Definition/Hypotheses

In their efforts to create an environmentally friendly method of detecting, quantifying and extracting the gold in ore, the 2017 Ashesi iGEM team used a pair of fluorescent proteins (known as FRET) to tackle the detection and quantification bit. However, with the low yield of bacteria and in effect, low protein production, the device was not as effective as it was designed to be. The team chalked this occurrence to the lack of a standard laboratory incubator.

However, recent studies have shown that bacterial growth is not just affected by the commonly known biological and chemical environmental factors; mechanical stimuli can also be a factor of optimal bacterial growth [5]. For decades, the surfaces or the fluids that bacteria grow in have been ignored when describing their growth; now recent advances in technology have shown that bacteria are attuned to mechanical forces in their environment and can exploit these mechanical stimuli to drive adaptive behavior [6].

The dependence of protein production on bacterial growth has long since been established [7]. Barring all other factors, the higher the number of bacteria in solution, the higher the yield of protein in the cells.

Based on the conclusion drawn above, mechanical stimuli affect bacterial growth and in effect protein production and this project sets out to validate this statement.

1.5.Significance of Project

Microbe based biosensors are replacing the other categories of biosensors due to their relatively high stability, fast replication of the micro-organism and the ease of engineering (from synthetic biology principles). This project will therefore provide a better understanding on the conditions under which biosensors work and how to manipulate these

conditions to increase the performance of microbe-based biosensors that use bacteria as their micro-organism of choice.

Also, this project will contribute to existing research that proves the importance of factoring mechanical stimuli into bacterial growth mathematical models.

1.6.Project Scope

This project will focus primarily on the formulation of a mathematical model that includes the effect of mechanical stimuli on bacteria growth . A platform will be designed and built to implement experimental phase of the project . If this phase is successful, then the design of a portable whole cell biosensor specific to the iGEM 2017 project will be developed.

If these phases are completed, the project will further perform a calibration experiment for the fluorescence measurement of the red fluorescent protein against protein production in the bacteria.

1.7.Thesis Chapter Outline

Chapter one constitutes the main introduction to the problem and the project (background information, problem definition, aims and objectives of the project, expected outcomes of the project, hypotheses, the significance of the project, research methodology, project scope, and the chapters outline).

Chapter two is the overview of biosensors and the gaps in biosensor knowledge that make this project worth doing (from literature review).

Chapter three comprises the design decisions and the materials and methodology of the project.

Chapter four centers on the implementation of chapter 3 and how it differs from the design decisions captured in Chapter 3.

Chapter five focuses on the results of implementation

Chapter six presents the discussion of results, summary and conclusion of the project.

Chapter 2: Literature Review

2.1.Overview

This section provides a more detailed look into biosensors and its ties to synthetic biology as well as the limitations of biosensors as well as its significance that make it worth looking into.

2.2.Synthetic Biology and the Use of Biosensors

The Secretariat of the Convention on Biological Diversity suggests that there is no internationally accepted definition of synthetic biology [8]. It can however be broadly defined as the engineering of biological systems for novel functions. [9]. The applications of synthetic biology are endless; from biomedical research to monitoring and treatment of diseases to environmental remediation. However, biosensors have come to represent the idea of synthetic biology due to their versatile application in multiple different areas such as biomedical, environmental and even computing applications. Simply put, we define biosensors as devices that can convert biological responses into measurable signals.

Biosensors have been used ever since 1962, when Leland C. Clark invented the first biosensor for oxygen detection [10,11]. Since then, different types of biosensors have been invented and implemented. Biosensors typically involve a:

- Target analyte – The substance of interest to be detected [10].
- Bio-element – Molecules that specifically recognize and interact with the target analyte resulting in biochemical reactions. Enzyme, antibodies, nucleic acids, cells, etc. are examples of commonly used bio-elements in biosensors [10,11].
- Transducer – The element that convert the biochemical reaction into measurable signals. Methods of transduction include electrochemical, electrical, optical, piezoelectric, etc. [11].

- Signal – The signal from the transduction stage can be either digital or analog. Based on the type of user interpretation system used, some biosensors involve either A/D or D/A converters. The signal obtained can be represented as audio, or as a chart. [10].

The basic operation of a typical biosensor is summarized in Figure 2.1, depicting specific detection of the analyte and transforming it into a signal which can be processed by different signaling processing units. As with the typical parts that every biosensor has, there are also some common attributes that all biosensors possess.

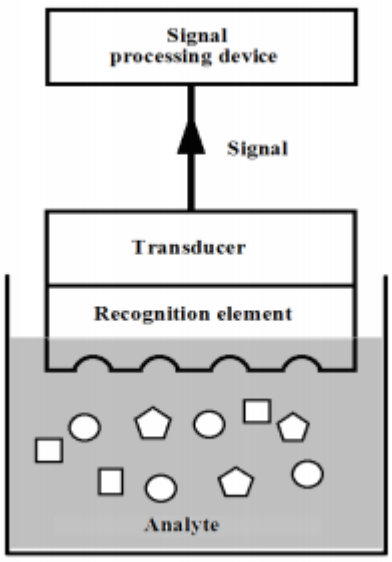

Figure 2.1: Typical operation of typical Biosensors [14]

- Selectivity – The ability of the bio-elements to recognize the target analyte in a mixture of contaminants and other compounds [10].
- Reproducibility – The ability of a biosensor to produce identical responses/measurements to identical experimental setups. The reproducibility of a biosensors is to a large extent dependent on the precision and accuracy of the transduction elements [10].

- Stability – Refers to the degree of susceptibility of a biosensor to the changes in its environment. When a biosensor is affected by ambient disturbances, it can cause errors in measurement values that can affect its precision and accuracy [10].
- Sensitivity – The minimum amount of target analyte that a biosensor can detect [10].
- Linearity – The ability of the measured response of a biosensor to be accurately represented on a straight line, i.e. $y = mx$, where y is the output signal, m is the sensitivity of the biosensor and x is the concentration of the target analyte [10].
- Quick response and recovery times – The response time of a biosensor is the time from the detection of the signal by a biosensor to the relay of measurements to its transducer components. Fast response times equals effective data monitoring [12]. After measurement, the time it takes the biosensor to revert to its original state represents its recovery time. Fast recovery times results in sensors that are re-usable [12].

Biosensors can be classified into different categories based on their specific operations; i.e. what specific principles guide their basic operations (seen in Figure 1). The first category of biosensors is based on transduction methods, including electrochemical, optical, piezoelectric, thermometric, ion-sensitive, magnetic, etc. [11]. Another classification of biosensors is on the biorecognition principle: biocatalytic group usually including enzymes, bio-affinity group, which usually antibodies and nucleic acids and the microbe-based group, whose functionality is based on changes in specific features of a microorganism [2]. As mentioned in Chapter 1, microbe-based biosensors are generally preferred to the other types of biosensors due to their intrinsically modular design .

Whole-cell biosensors are a type of microbe-based biosensors whose recognition element is usually a living cell. Common micro-organisms used in whole cell biosensors can either be prokaryotic or eukaryotic including yeast, fungi, bacteria, plant tissue cells,

etc. Changes in the organism's cellular metabolism, pH and gene expression are usually quantified as a response to the target analytes for whole-cell biosensors [13]. In comparison to catalytic biosensors, whole cell biosensors are crudely and primitively referred to as a bag of enzymes because of their similar operations [14]. The main advantage of a whole-cell biosensor over a catalytic biosensor is its generality [15]. Catalytic biosensors tend to target specific analytes; they cannot be used to ever detect anything else. Whole-cell biosensors, however, can be engineered to respond to a variety of target analytes, hence its crude name, bag of enzymes. Furthermore, the organisms mentioned above are all naturally occurring. Therefore, the selection of a specific organism for the biosensor is dependent on the environment of the target analyte. Despite their many advantages, whole-cell biosensors have two main disadvantages: a slower response time than their catalytic counterparts and a somewhat controlled selectivity. Whole cell biosensors tend to have a many more enzyme as compared to the single enzyme extracted for catalytic sensors and this tends to affect the selectivity of the biosensor [14].

2.3.Gaps in Current Knowledge

The use of bacteria in whole-cell biosensors has recently become very common, especially in sensors that have been genetically modified [15,16]. However, bacterial responses to chemical and biological stimuli has been a subject of study for many decades and is therefore well-understood [4]. Other areas have been neglected, such as the study of bacterial responses to mechanical stimuli among others [4,6]. It is an inescapable fact that most bacteria grow on a myriad of surfaces; on or in various fluids. For instance, it is a common practice to culture bacterial cells on LB and agar plates or in LB broth solutions. The shear stresses induced by fluid flow, cell-to-cell contact, and cell-substrate contact can all affect the chemical and biological cues of bacterial physiology as seen in Figure 2.2 [4]. It is observed that gene expression is one of the areas that can be affected by mechanical

stimuli. It was mentioned earlier that one of the main disadvantages of whole-cell biosensors is its low selectivity. Selectivity of a biosensor is affected by protein production which is in turn affected by gene expression [7]. Therefore, bacterial whole-cell biosensors can be affected by mechanical stimuli. If bacterial responses to mechanical stimuli are optimized, bacterial whole-cell biosensors can also be optimized, and their selectivity improved.

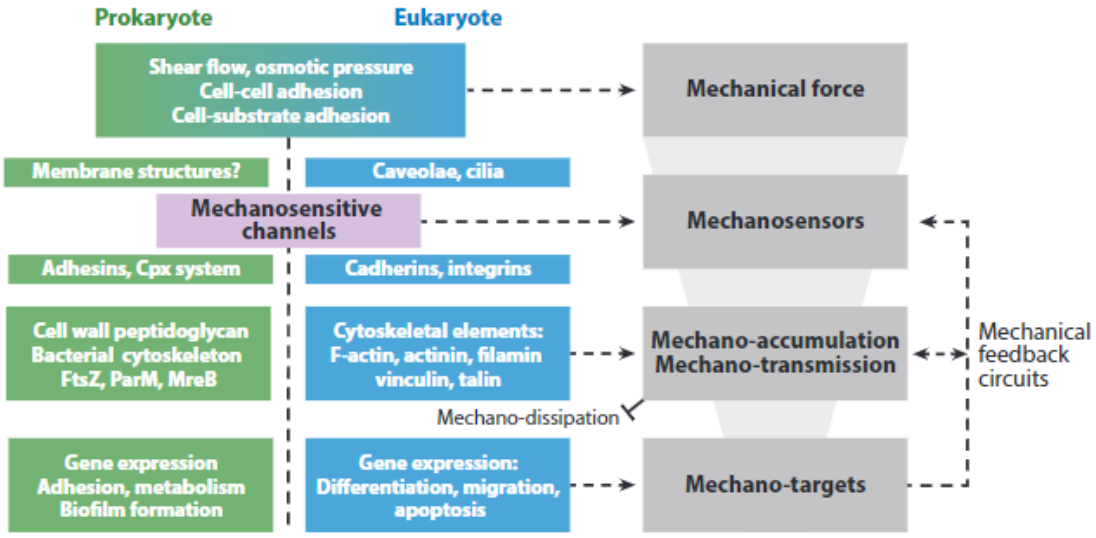

Figure 2.2: Mechano-transduction in both prokaryotes and eukaryotes

2.4.Project Fit and Outputs

Based on the literature review: mechanical stimuli affect bacterial growth and this project sets out to validate this statement. Bacterial responses to mechanical stimuli is an underexplored subject, the hypothesis formulated in the previous sentence has no research backing; very little has been done on this subject to ensure its validation and this project will therefore contribute to the understanding of the changes in bacterial behavior due to bacteria mechanics as well as the existing research on biosensors. If proven true, this hypothesis could increase the impact of biosensors in food processing, environmental remediation and many other synthetic biology applications. Aside the contribution to existing literature, one of the main project outputs is a physical incubator with a robot that varies the direction of motion of the platform containing the bacteria.

Chapter 3: Design

3.1. Overview

This chapter provides an overview of the requirements of the product to be developed and how it compares to existing products of similar functions.

3.2.Review of Existing Designs

3.2.1. Laboratory Microbiological Incubators

Laboratory microbiological incubators are devices that provide the optimal conditions for the growth of microbiological cell cultures [17]. For *E.coli*, one of the most commonly used organisms in research laboratories, 37℃ is the optimal temperature for growth [17]. Some other microbes may require a certain pH which requires the use of a CO_2 incubator, some require a certain amount of humidity or even different temperature ranges.

Most incubators either employ natural or forced convection to avoid temperature gradients and have LCD's to display the conditions in the incubating chamber. Most also have alarms to inform users of deviations in the conditions the incubating chamber. However, most standard laboratory microbiological incubators do not provide the optimal mechanical conditions needed for bacteria growth, because not much is known about their effect on bacteria. The few that do are known as shakers. Shakers have oscillating boards that are used to agitate substances in a tube or a flask [18]. Shakers can be used for a few minutes to agitate a substance, or as shaking incubators that perform the same function as a standard micro-biological incubator while eliminating the need for cultures that need to be shaken and incubated at the same time [18]. However, the nature of shaking for these incubators is an oscillating type of movement [18]. The purpose of this type of movement is to increase the rate of oxygen transfer (OTR), which increases the amount of "resources"

that the bacteria being agitated have [18]. Although the shakers are quite different from the movement type to be implemented in this project, they are a very close comparison. The average laboratory micro-biological incubator costs about $3000 [19].

3.2.2. Micro-Incubators

Given that POCD such as biosensors are used in areas without laboratories and trained personnel, portable micro-incubators have been designed to support environmental monitoring and remediation [20]. *E.coli* is one of the most common indicators used in genetically engineered biosensors and most micro-incubators are designed to culture these micro-organisms[21]. Most micro-incubators feature the exoskeleton of most microbiological incubators: an outer casing with further insulation, a temperature control mechanism and a display (to project the conditions of the incubating chamber). Outer casings can be 3D printed, fabricated from wood, etc. and further insulated to prevent heat loss. The temperature control mechanism includes a temperature sensor whose measured values are passed into a micro-controller acting either as an on/off controller or a PID controller to adjust the temperature if the temperature recorded is outside the tolerance level. The tolerance of most micro-incubators due to the simplicity is usually $\mp 3℃$ [22]. Some temperature control mechanisms include a fan to prevent temperature gradients from occurring and to ensure even temperature distribution. More often, the display is linked to the micro-controller which reads the values from the sensors and projects onto the display. PID controllers, however, will provide a much more precise temperature control mechanism, as they “auto-correct” the system continuously, instead of waiting for the incubating chamber to heat up or cool down to the desired temperature as on/off controllers are prone to do.

Therefore, portable micro-incubators that use PID controllers instead of on/off controllers will function as well as microbiological incubators without costing as much standard laboratory microbiological incubators [23].

3.3. Overall Product Description

The Alpha platform, the main output of this project, is to provide optimal conditions (mechanical and temperature control) for the growth of *E.coli* genetically engineered to include a generic red fluorescent protein. The addition of the red fluorescent protein is to provide an easily measurable indicator on how the growth of the bacteria has improved using the platform. The increase in color intensity is directly proportional to the bacteria population. Figure 3.1 shows a graph that proves this relation.

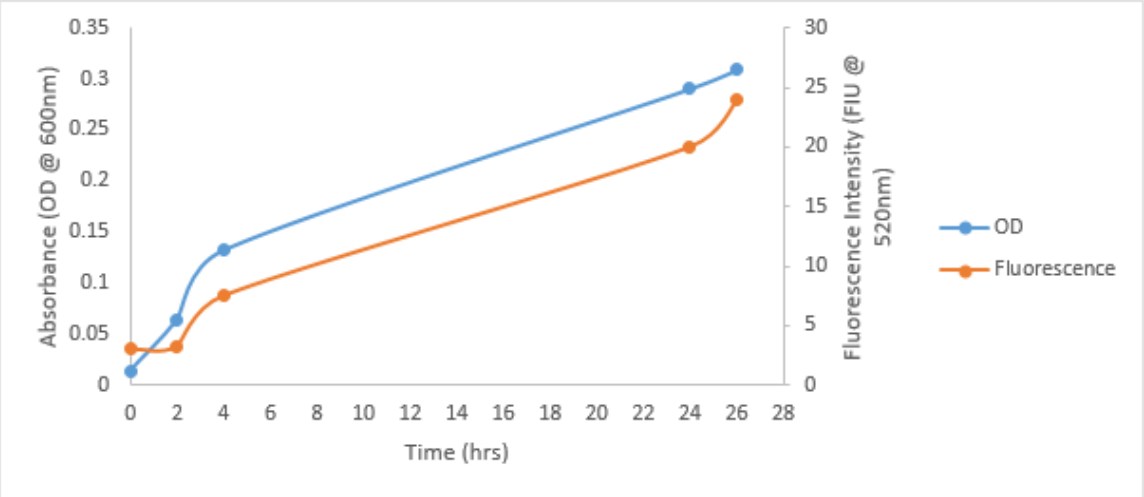

Figure 3.1: Graph of fluorescence and absorbance of an E.coli colony carrying a fluorescent protein against time

Since the alpha platform is to provide the conditions necessary for the growth of the bacteria, it is to function as an incubator. Unlike shaking incubators, the Alpha platform is not limited in the type of movement it exhibits. It includes an enclosure made from wood and insulated with Styrofoam. The movement types are performed by the adapted Delta robot which is placed in the enclosure. This is an important change as it will allow to the researchers to investigate the effect of mechanical stimulation on bacterial growth.

Although the intention was to design the Alpha platform as POCD, due to the constrains in manufacturing of the prototype, this 1st generation will not be categorized as POCD as it is not portable which is major characteristic for POCDs but it will inform the future design of the next generations as POCD for biosensors [24].

3.4.Design Decisions

3.4.1. Project Schedule

For an effective management of the prototype manufacturing it is important to divide the project into manageable sections and apportion time to each of the tasks that need to ensure that each phase is carried out on time. The project schedule can be seen in Figure 3.2.

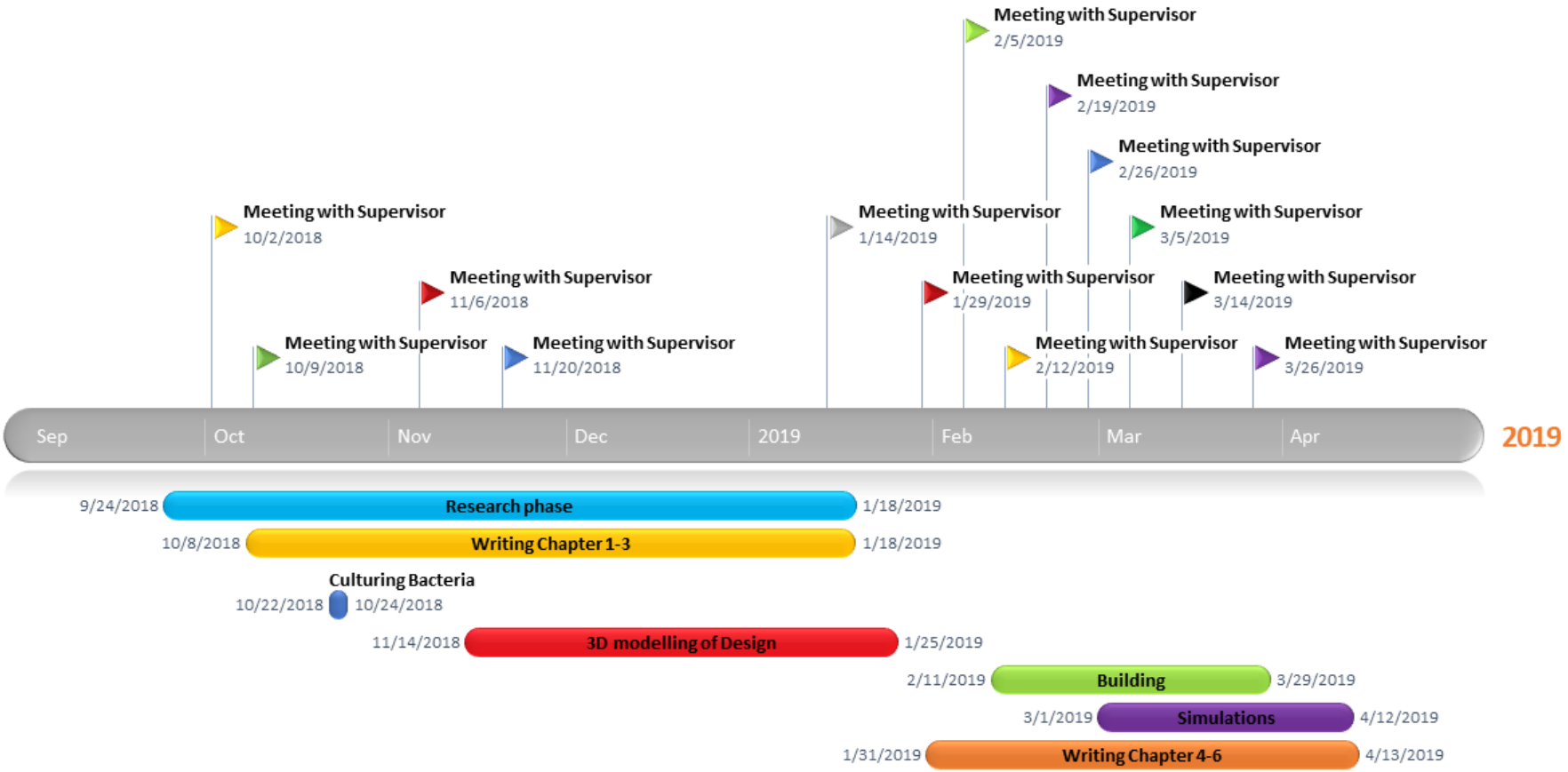

Figure 3.2: Proposed Project Schedule

3.4.2. User Requirements

Apart from determining the effect mechanical stimuli have on protein production and bacterial growth in whole cell biosensors, the Alpha platform will inform the design of a portable biosensor to be used in the detection and quantification unit of future Ashesi iGEM projects. It is proposed that for the iGEM 2017 project [25], the Alpha platform will serve as a POCD for the biosensor, enabling quantification of gold on site. The user requirements of the Alpha platform are as follows:

- Affordable – The Alpha platform must be designed with readily available and affordable materials to reduce its overall cost.
- Rapid and Robust – The Alpha platform should be able to run without continuous intervention from its user. It should also be reusable without needing much maintenance or repairs.
- User-Friendly – The Alpha platform should require very little training to operate.
- Versatile – The Alpha platform should be able to be integrated (with little to no additional work) into a wide variety of applications that need portable micro-incubators.

The POCD's user requirements will be described by the ASSURED criteria, **A**ffordable, **S**ensitive, **S**pecific, **U**ser – friendly, **R**apid and **R**obust, **E**quipment Free, **D**eliverable to end user [26].

3.4.3. System Requirements

- The Alpha platform should be capable of running for at least 24 hours to ensure bacteria run their incubation period without stops.
- The temperature of the incubating chamber must be kept at 37℃ with ∓2℃ tolerance. The design of the incubator should therefore feature a PID controller.

- The maximum load the Alpha platform can support should not be more than 805.8g. The determination of this can be seen Chapter 3.5.2.
- The Alpha platform must be able to display the temperature of the incubating chamber and give a warning when temperature exceeds or falls below the threshold set.
- The tray holding the tubes should be easily accessible.
- The incubator should take at most, 5 minutes to reach the desired temperature tolerance.
- The steady state error of the incubator for a unit step input ≤ 0.05.
- The incubator should have a maximum overshoot temperature of 45℃ [17]. The maximum percent overshoot of the system can be calculated as: $(PO\%) = \frac{Y_{max}-Y_{ss}}{Y_{ss}} * 100\% = \frac{45℃-37℃}{37℃} * 100\% = 21.62\%$. However, using a design factor of 2, then the maximum percent overshoot of the system should be $10.81\% \cong 11\%$.

3.4.4. Pugh Matrix

The Pugh Matrix is a type of Design Matrix that aids in the design decision process by comparing various designs as against a set of criteria specified by the designer, ultimately leading to the design that best meets the set criteria [27].

Table 3.1: Pugh Matrix, where, 0 = same, + = better and - = worse

Evaluation criteria	Weight - 5 is high	Reference Design: Microbiological Incubators	Concept 1: Shaking Incubators	Concept 2: Portable Micro-Incubators
Affordable	5	*0*	*0*	*+5*
Rapid and Robust	5	*0*	*0*	*+5*
User-Friendly	4	*0*	*0*	*+4*
Versatile	3	*0*	*0*	*0*
Temperature Control	3	*0*	*0*	*0*
Total Score		*0*	*0*	*14*

3.5. Design Process

With the aim of trying to determine how mechanical stimuli affect bacteria, the Alpha platform provides a method to vary speed and direction of motion and such bacteria will be exposed to forces of different directions and magnitude. The first choice considered to accomplish this was a robot arm (serial manipulator). However, this was quickly dismissed due to the complexity necessary to produce the code required. The next approach considered was two universal joints coupled with a gear train, however, this would provide limited degrees of freedom. The final choice, which is the implemented design, is the adaptation of a delta robot, which is often used in most industrial settings for its high precision and speed. The main reasons behind it being the most preferred choice out of the others were:

- Larger degrees of freedom
- Ease of coding (simpler than the robot arm)
- Versatility (in terms of its end effector). The end of effector of the delta robot can be more easily changed to suit whatever purpose than the robot arm.

3.5.1. 3D Model Iterations

The first iteration of the delta robot in the Alpha platform is as seen in Figure 3.3. SolidWorks by Dassault Systems was used to model all designs.

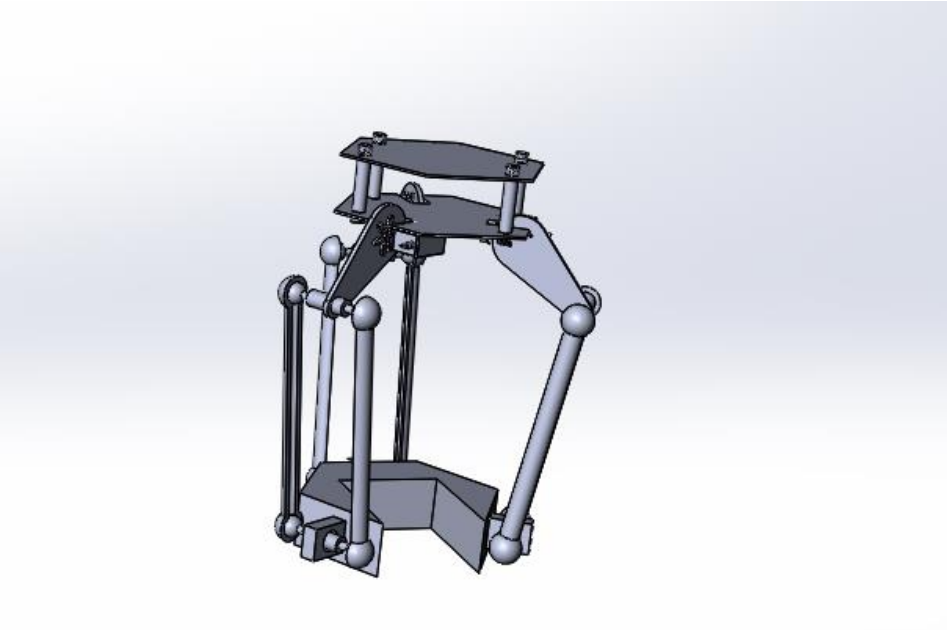

Figure 3.3: First design iteration

This design was found to have a lot of design constraints and therefore was impractical to be built. The second and final iteration of this is as seen in Figure 3.4.

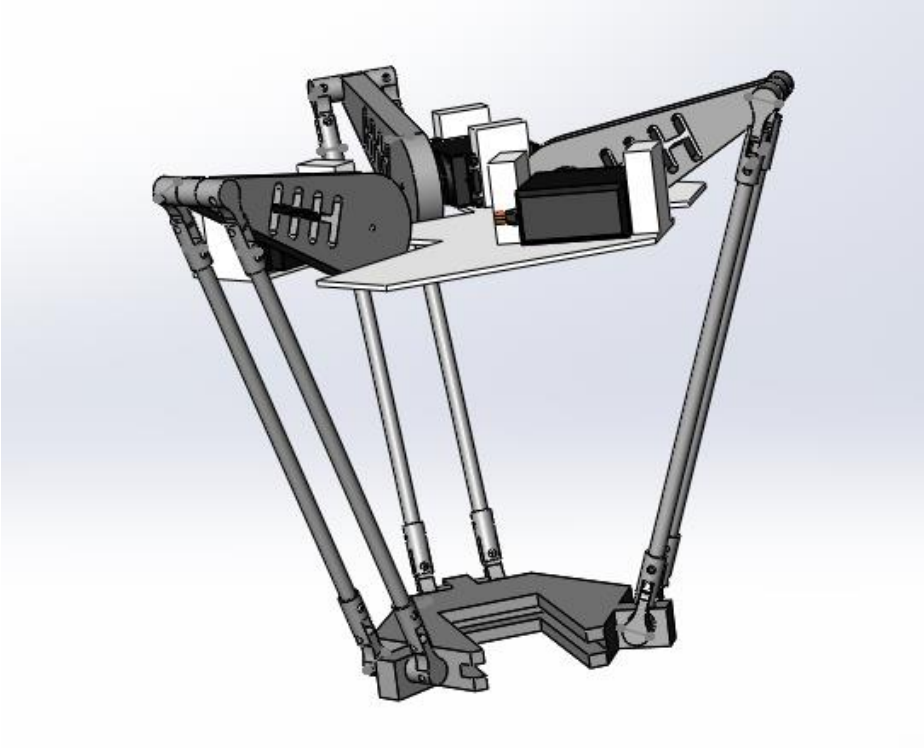

Figure 3.4: Final design iteration

The enclosure of the Delta robot is as seen in Figure 3.5.

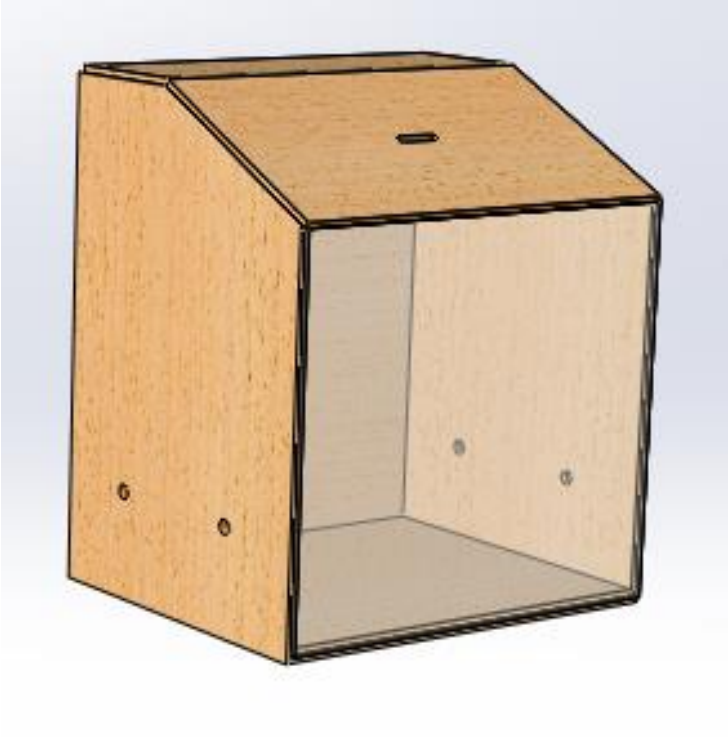

Figure 3.5: Incubator enclosure

3.5.2. Kinematics of the Adapted Delta Robot

Perhaps the most important part of designing the delta robot is the kinematic modelling. Kinematic analysis is an essential component for motion control [28]. This analysis can be done two ways: direct or inverse kinematics. For the purpose of this project, the inverse method will be used as it is the easier of the two methods [28]. The inverse method involves the determination of the position of the end effector by calculating the motor angles. This aids in the control of each motor based on the application the robot is to be used in.

The delta robot can be simplified as seen in Figure 3.6.

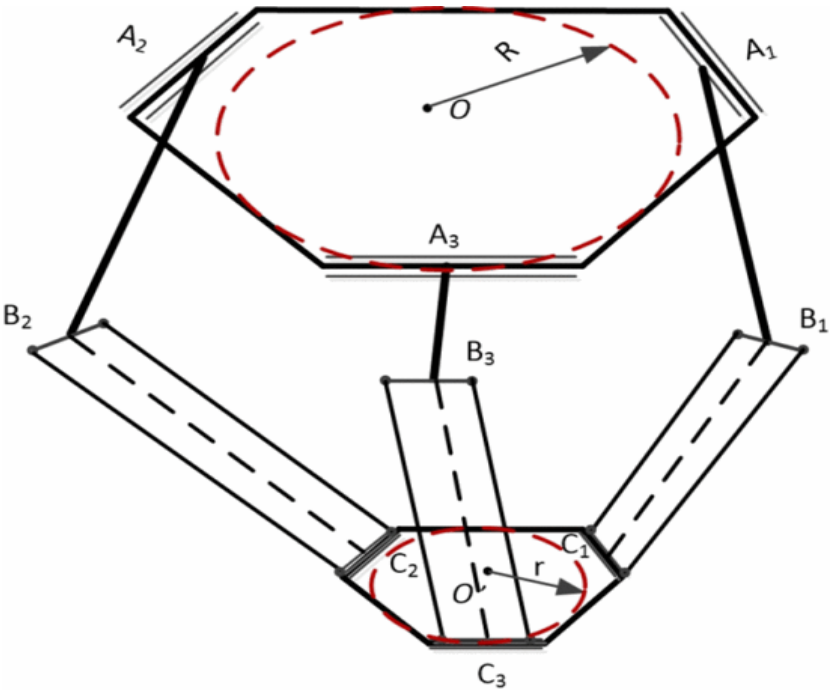

Figure 3.6: Simplified model of the delta robot [29]

As is, the system has three translational DOF's. Let the segment between A and B be known as the bicep and that between B and C be known as the forearm. A hypothetical segment can be added to the center of the forearm, given the designation i, to represent each joint, where $i = 1,2,3$. R and r represent the radii of the base and end effector respectively.

Each motor is positioned at $A_1, A_2\ and\ A_3$ and will follow the co-ordinate system seen in Figure 3.7.

A base plane can now be created by placing the vertices of a triangle on the z axis of each motor, where the centerline is perpendicular to each z axis. The origin of this base coordinate system will be located at the center of the imaginary triangle with $+Z$ pointing away from the base plane and $+X$ being coincident with the centerline of the imaginary triangle (as seen in Figure 3.7).

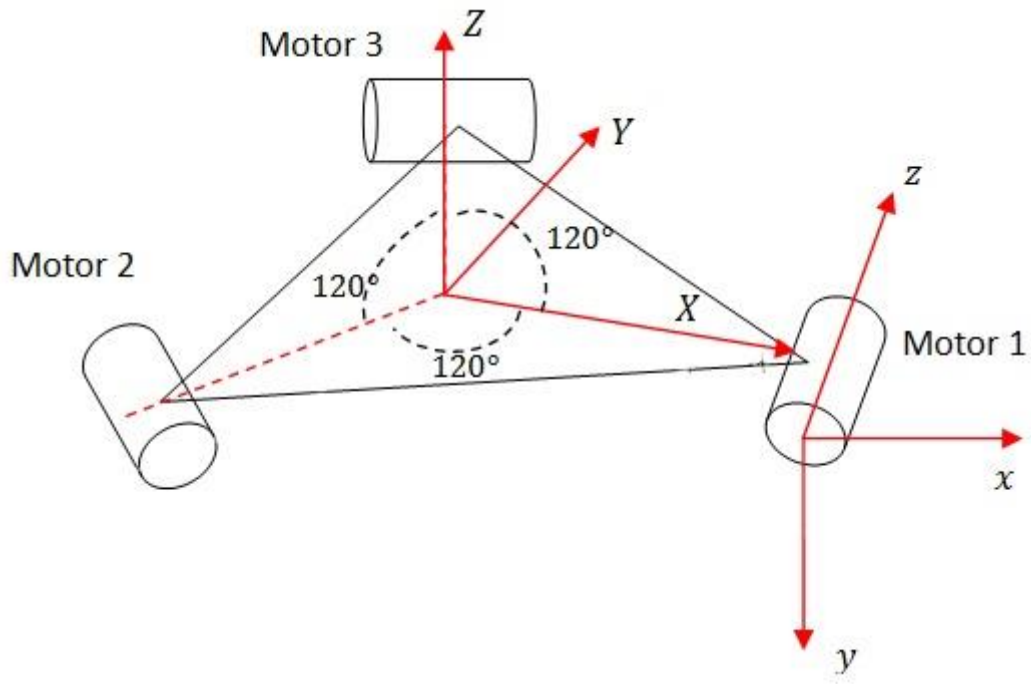

Figure 3.7: Base and motor coordinate frames [29]

The rotational axis of each motor is along the $z - axis$ and each bicep will rotate in the xy plane. Determining coordinate frames for the Denavit-Hartenberg method relies on the following rules:

- The $z - axis$ of the ith joint is in the direction of said joint axis. For a revolute joint, this is its rotational axis.
- The $x - axis$ of the ith joint is perpendicular to both the z_I and z_{i-1}. However, if there is no unique perpendicular axis, then x_i goes in the direction from z_I and z_{i-1}.

- $z - axis$ must follow the right-hand rule seen in Figure 3.8

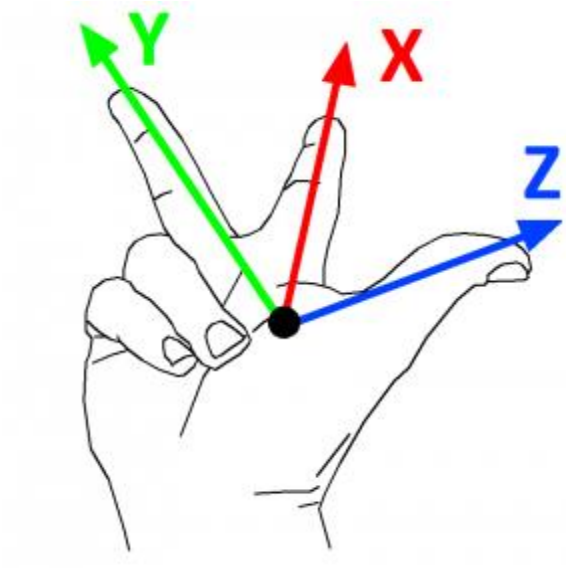

Figure3.8: Right hand rule representation for axis orientation[30]

- The x_i axis must intersect with the z_{i-1} axis

Based on these four rules, the motor coordinates can be seen in Figure 3.9.

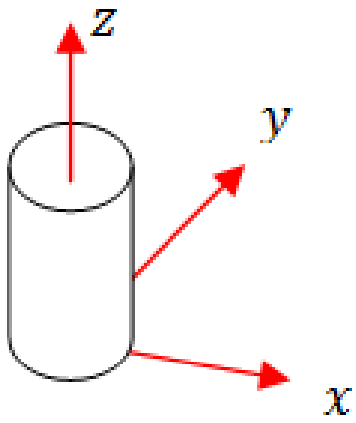

Figure 3.9: Motor coordinate frame [29]

From Figure 3.10, it is observed that z_{i-1} and z_i are parallel, meaning that both axes will have an infinite number of normal vectors, so any one of them can be chosen to be x_i. For easy calculations and reference, x_i was picked so that it passes through o_{i-1}. An

imaginary line is drawn from z_i to z_{i-1} through o_{i-1}. The point where the imaginary line intersects z_i becomes o_i and x_i goes through o_i in the direction of the imaginary line.

With each ith joint, the joint variable associated is as follows:

$$q_i = \begin{cases} \theta_i, if\ joint\ i\ is\ revolute \\ d_i, if\ joint\ i\ is\ prismatic \end{cases} \qquad (1)$$

$$\therefore If\ joint\ B\ is\ the\ ith\ joint\ to\ be\ considered, q_{i-1} = A_i$$

Since each joint is revolute, the joint variable is simply reduced to:

$$q_i = \{\theta_i \qquad (2)$$

To aid in the determination of the motor angles, a known base coordinate must be converted to motor coordinates. And to align a base coordinate to a motor coordinate, Denavit – Hartenberg transform will be used to provide a transform matrix that can yield a motor coordinate from the end effector position in base coordinates.

Let X_i represent the homogenous transformation that gives the position and orientation of each ith link with respect to the $ith - 1$ link, which changes as the robot moves.

There are four Denavit - Hartenberg parameters needed to compute the motor angles. They are as seen in Table 3.2.

Table 3.2: Denavit Hartenberg parameter table [30]

Parameter	Description
$\boldsymbol{\alpha_i}$ (Link twist)	Rotation angle between z_{i-1} and z_i about the x$-axis$ of the ith joint
$\boldsymbol{\theta_i}$ (Joint angle)	Rotation about the $z - axis$ of the $ith - 1$ joint if said joint is revolute
$\boldsymbol{d_i}$ (Link offset)	Translation between two coordinate frames along the $z - axis$ of the $ith - 1$ joint if said joint is prismatic
$\boldsymbol{a_i}$ (Link length)	Translation between two coordinate frames along the $x - axis$ of the ith joint

The parameter values corresponding to one of the three arms of the robot are as seen in Table 3.3.

Table 3.3: Denavit Hartenberg Parameter Values

$\boldsymbol{i}$	$\boldsymbol{\theta}$	$\boldsymbol{\alpha}$	$\boldsymbol{d}$	$\boldsymbol{a}$
1	θ_1	$-90°$	0	0.06
2	θ_2	0°	0	$L_b, length\ of\ bicep$

To simplify the model, the assumption made is that X_i is a function of the scalar joint variable. The homogenous transformation that expresses the position and orientation of the ith link with respect to the $ith - 1$ link is as follows:

$$X_i = [R_z(\theta_1)T_z(d_1)T_x(a_1)R_x(\alpha_1)][R_z(\theta_2)T_z(d_2)T_x(a_2)R_x(\alpha_2)]$$
$$\dots [R_z(\theta_n)T_z(d_n)T_x(a_n)R_x(\alpha_n)] \qquad (3)$$

$$where\ T\ represents\ translation\ and\ R\ represents\ rotation$$

These four parameters concisely describe the robot concisely. These four parameters change as the robot moves and these calculations will be difficult to keep track of by hand. A MATLAB script (in Appendix A) describes these parameters and the control of the robot. Using the calculation below, it was determined that the maximum load the platform can carry is $805.8g$.

Figure 3.10: Free-body diagram of maximum load estimation [29]

To find the maximum weight that the Delta robot can support, we can assume that when the bicep is at 0°, all the forces acting on the robot act vertically downwards. Therefore:

$$\sum F = mg = (M_b + M_f + M_e)g \qquad (3)$$

$$where\ M_b\ is\ the\ mass\ of\ the\ bicep$$

$$M_f\ is\ the\ mass\ of\ the\ forearm$$

$$M_e\ is\ the\ mass\ of\ the\ end\ effector/load$$

$$\sum M = \frac{mg}{g} = (M_b + M_f + M_e) = \rho_b V_b + \rho_f V_f + M_e \qquad (4)$$

$$\sum M = (0.01m * 0.11m * 0.03m) * (\frac{1250kg}{m^3})) + ((\frac{1250kg}{m^3}) * \pi * \frac{0.006^2}{4} * 0.213m) + M_e$$

$$\sum M = 0.8545kg$$

$$but\ \tau = \sum F * r = \sum F * L_b \qquad (5)$$

$$where\ L_b\ is\ the\ length\ of\ the\ bicep$$

$$\tau \leq \frac{9.40kg}{cm}$$

$$\therefore \frac{9.40kg}{cm} \geq \sum M * L_b$$

$$\frac{\frac{9.40kg}{cm}}{11cm} \geq M_e + 0.8545kg$$

$$\therefore M_e \leq 0.805767kg$$

3.6. Materials

3.6.1. Material Selection Process

As seen from the final design in Figure 3.4, the Alpha platform can be categorized into two main groups, the adapted Delta robot and the outer casing. Given that the materials to construct the platform must be readily available and cheap to fulfill the Affordable criteria, the outer casing is to be made from wood (plywood) and further insulated with Styrofoam. To determine if the wood and Styrofoam are suitable for this application, the maximum service temperature must be known. The maximum service temperature of a material is the maximum temperature above which a material's properties significantly degrade over time.

The adapted Delta robot to be used in the incubating chamber of the Alpha platform is almost entirely 3D printed; the 3D printed parts would be PLA based. The maximum service temperature of PLA like the wood and Styrofoam must be above 37℃. Given that the incubating temperature is to be 37℃ with $\mp$2℃ tolerance, PLA with its maximum service temperature range from about $45℃ - 58℃$, seen in Figure 7, is suitable for use in the Alpha platform. Wood and polyurethane foam also fit the criteria with their maximum service temperature range from $120℃ - 140℃$ and $135℃ - 178℃$ respectively. The

minimum service temperature for PLA, wood and polyurethane foam fall below 0°C and can therefore be used in the Alpha platform. CES Edupak was used to generate both graphs in Figures 3.12 and 3.13 as well as determine the maximum service temperature.

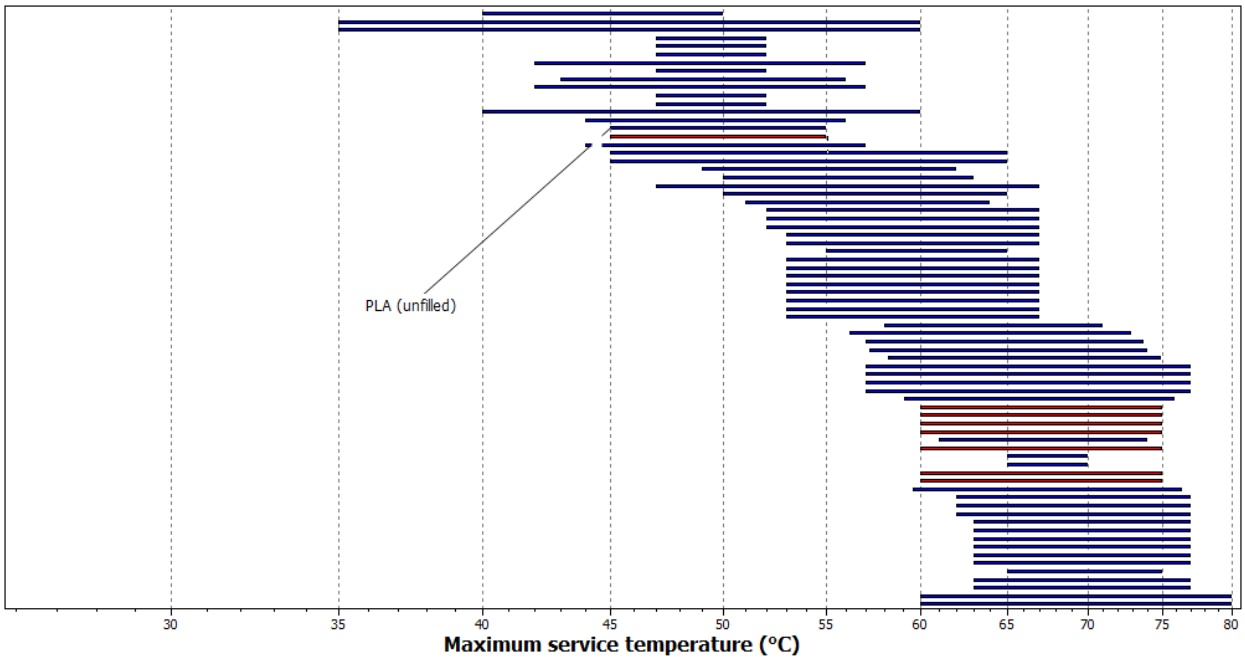

Figure 3.11: PLA Maximum Service temperature. Each bar represents a material and the differences in lengths along the x-axis is due to the range of their maximum service temperatures

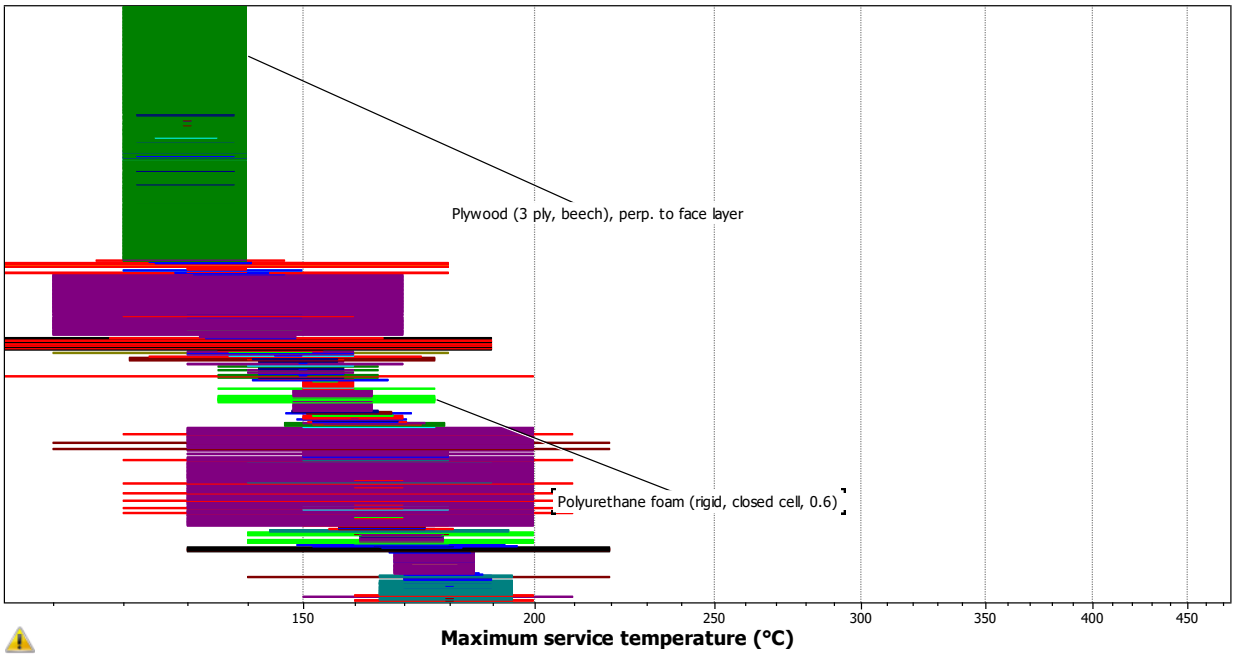

Figure 3.12: Plywood and Polyurethane foam maximum service temperature. This graph is the same as that in Figure 12. The only difference is the range of temperatures shown. The materials in this graph could not be viewed as thin bars because of the higher density of materials within this temperature range.

The thickness of polyurethane foam needed for insulation was calculated based on the following assumptions:

- There is steady state heat transfer through the walls of the incubator
- The temperatures of the outer surfaces of the incubator are equal and must be kept ≤ 30℃, i.e. heat transfer occurs along only the $x - axis$.

At steady state, the heat flow through the insulating material to the outside surface of the incubator = the heat flow from the surface to the surrounding air.

$$\therefore q_{insulation} = q_{surface} \qquad (6)$$

$$kA\frac{dT}{dx} = hA(\Delta T) \qquad (7)$$

$$dx = \frac{k}{h}\left[\frac{T_{incubator} - T_{surface}}{T_{surface} - T_{ambient}}\right] \qquad (8)$$

$$where\ k\ is\ the\ insulation\ material's\ thermal\ conductivity$$

$$but\ h = (10.45 - v) + 10\sqrt{v} \qquad (9)$$

$$where\ v\ is\ the\ speed\ of\ the\ fan\ in \frac{m}{s}$$

$$Given\ that\ the\ fan's\ lowest\ rpm = 1200rm$$

$$N.B. The\ fan's\ lowest\ rpm\ is\ used\ to\ ensure\ the\ maximum\ thickness\ is\ obtained$$

$$v = \frac{rpm}{60} * 2\pi * r \qquad (10)$$

$$where\ r\ is\ the\ radius$$

$$v = 2 * \pi * \frac{1200}{60} * \frac{0.075}{2} = \frac{4.7124m}{s} \qquad (11)$$

$$\therefore h = \frac{27.4456W}{m.K}$$

$$dx = \frac{0.050}{27.4456} * \left[\frac{37℃ - 30℃}{30℃ - 27}\right] = 4.25mm$$

Chapter 4: Experimental Methods and Implementation

4.1 Chapter Overview

This Chapter deals with how the design in Chapter 3 was implemented and how it differs from the design talked about in the previous chapter.

4.2 Implementation

The implementation of the proposed design was divided into three categories: Circuit, Code and Mechanical.

4.2.1 Circuit Implementation

The circuit schematic to control temperature in the incubator and the servomotors on the robot is as seen in Figure 14; it was generated by Fritzing. Fritzing is an open-source hardware initiative that aids in the development of electronic schematics and/or PCBs while allowing the user to simulate their circuits without having to build them.

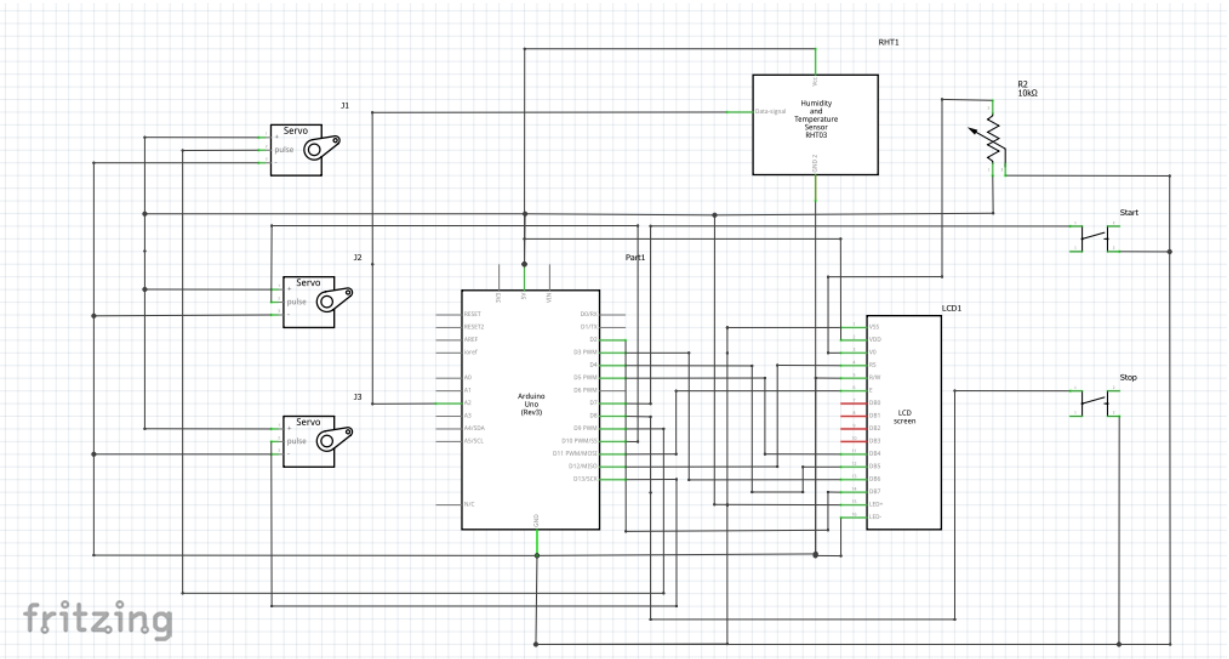

Figure 4.1: Circuit Schematic

The schematic in Figure 14 does not include the heater because Fritzing does not have a heating element in its library. The circuit schematic was implemented on a breadboard as this incubator is a prototype, not a final product. Figure 15 shows a picture of the actual circuit used in the incubator.

4.2.2 MATLAB/Simulink/SimScape/Arduino Implementation

For the temperature control in the incubator, there is the heat source and temperature sensor. To control the temperature of the incubator, the amount of heat provided by the heat source is controlled. Heat is provided by two 40W incandescent bulbs. For the purpose of this project, it was assumed that heat transfer in and through the incubator was by conduction and convection. A state space model for temperature inside the incubator (based on Figure 4.2) was constructed and the using the control system toolbox, the linear system analyzer was used to evaluate the system's response to a step input.

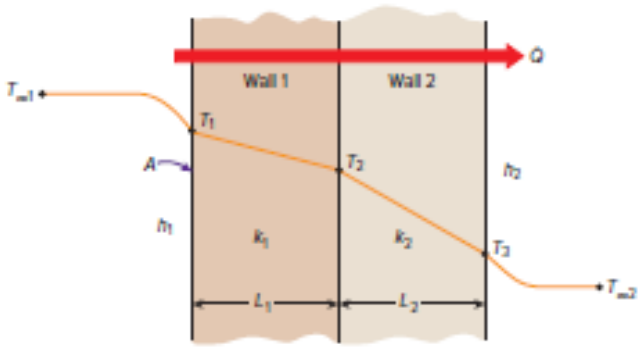

Figure 4.2: Cross section of incubator [31]

Where Wall 1 represents the Styrofoam and Wall 2 represents the wood.

The state space model parameters are as follows:

$$A = \begin{bmatrix} \frac{-h_i A}{\rho_a c_p v_i} & \frac{h_i A - \frac{k_1 A}{l_1}}{\rho_a c_p v_i} & 0 & 0 \\ \frac{h_i A}{\rho_1 c_1 v_1} & \frac{-h_i A + \frac{k_1 A}{l_1}}{\rho_1 c_{p1} v_1} & \frac{\frac{k_1 A}{l_1}}{\rho_1 c_{p1} v_1} & 0 \\ 0 & \frac{\frac{k_1 A}{l_1}}{\rho_2 c_{p2} v_2} & \frac{-\frac{k_1 A}{l_1} - \frac{k_2 A}{l_2}}{\rho_2 c_{p2} v_2} & \frac{\frac{k_2 A}{l_2}}{\rho_2 c_{p2} v_2} \\ 0 & 0 & \frac{\frac{k_2 A}{l_2}}{\rho_a c_p v_3} & \frac{-\frac{k_2 A}{l_2} - h_o A}{\rho_a c_p v_3} \end{bmatrix} \quad (12)$$

$$= \begin{bmatrix} \frac{-27.4456*0.25}{1.225*1005*0.015} & \frac{(27.4456*0.25)-\left(\frac{0.035*0.25}{0.05}\right)}{1.225*1005*0.015} & 0 & 0 \\ \frac{27.4456*0.25}{21*1215*0.0125} & \frac{(-27.4456*0.25)+\left(\frac{0.035*0.25}{0.05}\right)}{21*1215*0.0125} & \frac{\left(\frac{0.035*0.25}{0.05}\right)}{21*1215*0.0125} & 0 \\ 0 & \frac{\left(\frac{0.035*0.25}{0.05}\right)}{490*1700*0.00375} & \frac{-\left(\frac{0.035*0.25}{0.05}\right)-\left(\frac{0.13*0.25}{0.015}\right)}{490*1700*0.00375} & \frac{\left(\frac{0.13*0.25}{0.015}\right)}{490*1700*0.00375} \\ 0 & 0 & \frac{\left(\frac{0.13*0.25}{0.015}\right)}{1.225*1005*0.0125} & \frac{-\left(\frac{0.13*0.25}{0.015}\right)-}{1.225*1005*0.0125} \end{bmatrix}$$

$$= \begin{bmatrix} -0.37155 & 0.371552 & 0 & 0 \\ 0.0215 & -0.02206 & 0.000548697 & 0 \\ 0 & 0.000056022 & -0.0007496 & 0.0006936 \\ 0 & 0 & 0.14079 & -0.275466 \end{bmatrix}$$

$$B = \begin{bmatrix} \frac{\eta}{\rho_a c_p v_i} & 0 \\ 0 & 0 \\ 0 & 0 \\ 0 & \frac{-h_o A}{\rho_a c_p v_3} \end{bmatrix} \quad (13)$$

$$= \begin{bmatrix} \frac{0.8}{1.225 * 1005 * 0.015} & 0 \\ 0 & 0 \\ 0 & 0 \\ 0 & 1.225 * 1005 * 0.0125 \end{bmatrix} = \begin{bmatrix} 0.05415 & 0 \\ 0 & 0 \\ 0 & 0 \\ 0 & 0.13467 \end{bmatrix}$$

$$C = [T_i \quad T_1 \quad T_2 \quad T_3] = [1 \quad 0 \quad 0 \quad 0] \quad (14)$$

$$D = [0] \quad (15)$$

The temperature sensor used in this project is the DHT11 sensor. Both the heater and the sensor are connected to an Arduino Uno which functions as the microcontroller for this project. The code used to interface the Arduino with the sensor and heater can be found

in Appendix A. By using the MATLAB Support Package for Arduino Hardware, temperature is controlled in the incubator using a PID controller. Before this was determined as the best controller to use, PD and PID controllers were tested to determine if they yielded the correct desired system requirements: a settling time ≤ 2 minutes and an overshoot $\leq 11\%$. Table 4.1 shows the effect of K_p, K_i and K_d on a system.

Table 4.1: Effect of Kp, Ki and Kd tuning on a system [32]

Closed-Loop Response	Rise Time	Overshoot	Settling time	Stability
Increasing K_p	Decrease	Increase	Small Increase	Degrade
Increasing K_i	Small decrease	Increase	Increase	Degrade
Increasing K_d	Small decrease	Decrease	Decrease	Improve

The robot placed in the incubator is controlled by three (3) servomotors, each $120°$ apart. Using inverse kinematics, a MATLAB function was written to determine the joint angles based on the Denavit-Hartenberg parameters of the robot. The code can be found in Appendix A. Using the joint angles calculated, the robot is simulated in SimScape. Figure 4.3 shows a screenshot of the SimScape model used in simulating the robot.

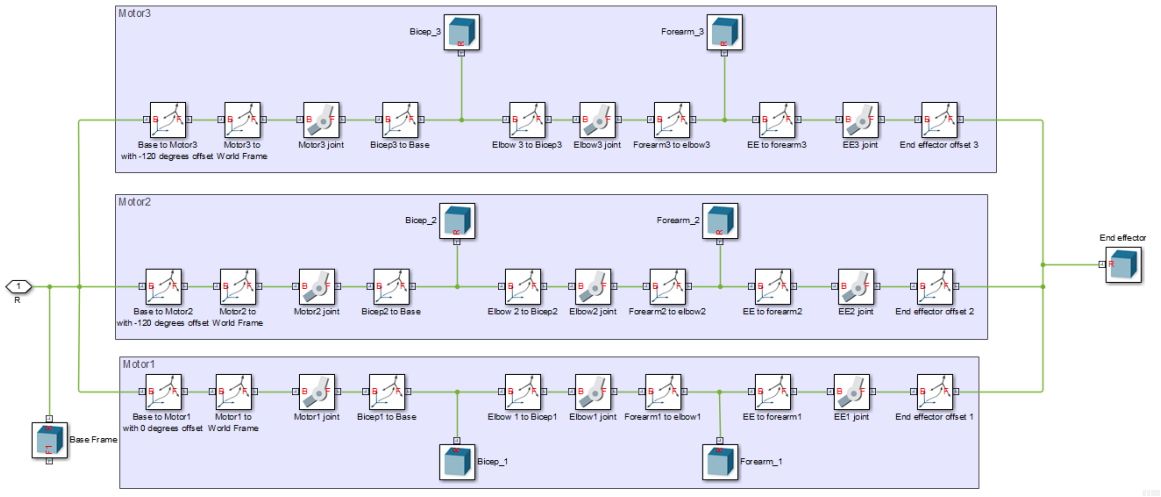

Figure 4.3: SimScape Model of Delta Robot for this project

4.2.3 Mechanical Implementation

The incubator enclosure was made from wood and insulated with Styrofoam. However, the Styrofoam thickness used was not the $5mm$ calculated in Chapter 3, but $5cm$. This was due to a miscommunication with the order placed for the Styrofoam. A picture of the finished incubator is as seen in Figure 4.4.

Figure 4.4: Incubator casing

4.2.4 Bill of Materials

In total, the cost of all materials used in this project is broken down in Table 4.2.

Table 1.2: Cost of Materials and Components used for this project

Material/Component	Unit Cost	Quantity	Cost
3D Printing filament	GH¢200.00	NA	GH¢200.00
Arduino Uno	GH¢70.00	1	GH¢70.00
DHT11 sensor	GH¢17.00	1	GH¢17.00
Plywood	GH¢20.00	NA	GH¢20.00
Plexiglass	GH¢30.00	NA	GH¢30.00
TowerPro servomotor	GH¢25.00	5	GH¢125.00
12V fan	GH¢7.00	1	GH¢7.00
40W incandescent bulbs	GH¢8.00	2	GH¢16.00
16x2 LCD	GH¢17.00	1	GH¢17.00
Breadboard	GH¢8.00	1	GH¢8.00
Pack of Jumper wires (male and female)	GH¢16.00	1	GH¢16.00
5V relay	GH¢11.00	1	GH¢11.00
Total			**GH¢537.00**

4.3 Method of Testing

Due to some technical malfunction the engineered organism was not available so biological testing was not performed, thus a mathematical model simulating the growth of the organism will be employed to demonstrate proof of concept.

4.4 Mathematical Model

4.4.1 Bacteria Transformation and DNA Uptake Process

To demonstrate the relationship between bacterial growth rate and protein production, the fluorescence produced by a red fluorescent protein was to be measured. As seen in Figure 3.1, it was expected that as the absorbance (indicator of bacteria growth) increased, the red fluorescence would increase. There were two main steps to achieve this: Transformation and then Plating and Inoculation.

- Transformation Process

  Competent cells are bacterial cells that have an increased possibility of taking up DNA than wild strains. The competent cells used were of the *DH5α* strain. The competent cells were shocked to ensure that the red fluorescent proteins were taken up by the cells. The red fluorescent proteins were placed in plasmids (a carrier of sorts) which had a chloramphenicol (antibiotic) resistance gene.

- Plating and Inoculation

  To ensure that only the transformed competent cells carrying the red fluorescent protein was used in further experiments, the cells were plated onto a chloramphenicol plate and left to grow overnight. All cells not carrying the red fluorescent protein die and all those who are live. A colony was then picked and inoculated into a tube of LB media

4.4.2 Model formulation

The purpose of the mathematical model is to forecast the effect of the robot movement on the bacteria. It is based on the estimation of the shear stress acting on each bacterium, which will be added as a term to the logistic growth curve (as seen in Equation 16).

$$\frac{dN}{dt} = rN\left(1 - \frac{N}{K}\right) \qquad (16)$$

Where N represents the current population as a function of time, r is the maximum growth rate, K is the carrying capacity and N_o is the initial population at $t = 0$.

The proposed model is as given in Equation 17.

$$\frac{dN}{dt} = rN\left(1 - \frac{N}{K}\right) * e^{-\frac{\tau}{r\dot{e}\varepsilon}} \qquad (17)$$

$$\tau = \mu\frac{v}{h} \qquad (18)$$

$$\dot{e} = \frac{\frac{dl}{dt}}{l} \qquad (19)$$

$$\frac{dl}{dt} = a\left(1 - e^{-\frac{t}{T}}\right) \qquad (20)$$

$$T = \frac{\gamma}{2k} \qquad (21)$$

Where τ is the shear stress acting on each bacterium, $\dot{e}$ is the elongation rate of each bacterium, μ is the viscosity of the media in which the bacteria is cultivated in, v is the velocity of the delta robot, h is the height of the media in the tube, l is the initial length of each bacterium, a is the linear rate of extension of the resting length of each cell, T is the time constant for the model, t is the time, γ is the intrinsic resistance parameter, k is the spring's constant of each bacterium and ε is the parameter that relates shear stress to elongation rate and growth rate. ε is the parameter to be varied.

4.4.1 Model Assumptions

- The shear force acting on each bacterium is assumed to be a uniformly distributed force.
- Each bacterium is oriented horizontally.
- Each bacterium is assumed to be an assembly of two independent halves, which expand symmetrically. Each cell half consists of a mass, m at the center of a semi-circular pole and are connected through a virtual spring with spring constant, k. This is as seen in Figure 4.5.

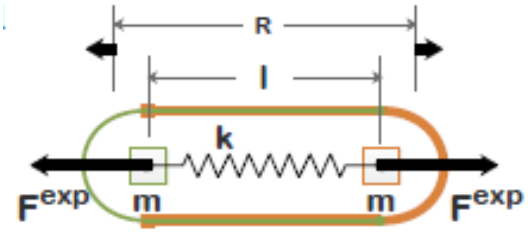

Figure 4.5: Spring model of E.coli [5]

- Each side of the platform is pinned.
- The LB broth is a Newtonian fluid
- Each bacterium is weightless
- The initial length of each bacterium is the same.
- The expansion rate of each bacterium is linear

Figure 4.6 shows a picture of a general logistic curve. It is expected that the term would increase the generation time of the bacteria, which is the exponential growth portion of the graph in Figure 4.6.

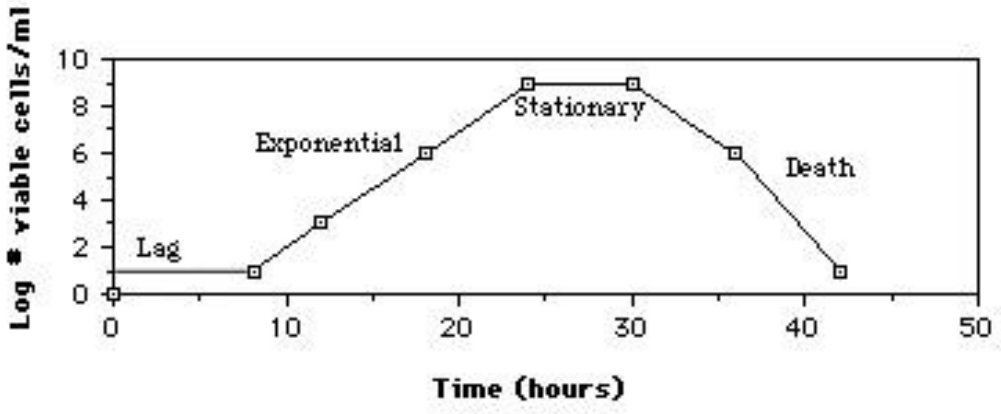

Figure 4.6: Graph depicting the phases of life of E.coli using a logistic model [33]

Chapter 5: Results

5.1.Temperature Control

It was determined from the linear system analyzer in MATLAB that the incubator thermal dynamics seemed to be of the first order. This was determined by computing a state-space model of the system. This was then converted to transfer function form using MATLAB's *ss2tf* function. However, the system has two inputs, the heater rating and the ambient temperature, and therefore two transfer functions. Of the two, only the transfer function relating the incubator temperature to the heater wattage was considered. The resulting transfer function is as seen in Equation 22.

$$\text{sys1} =$$

$$\frac{0.05415\ s^3 + 0.01615\ s^2 + 0.0003358\ s + 1.296e\text{-}07}{s^4 + 0.6698\ s^3 + 0.109\ s^2 + 0.0001003\ s + 1.949e\text{-}08} \qquad (22)$$

The transfer function shows that the system is of the fourth order. Figure() shows the graph of the system's response to a step input as well as the initial condition response. Figure 5.1 shows that the system seems to be of the first order. It can be seen in Figure 5.1

that the initial condition response of the system, starts from $T = 25℃$ and decays exponentially towards zero, meaning that the system is stable. Moreover, all the poles of the system are negative, alluding to the stability of the system.

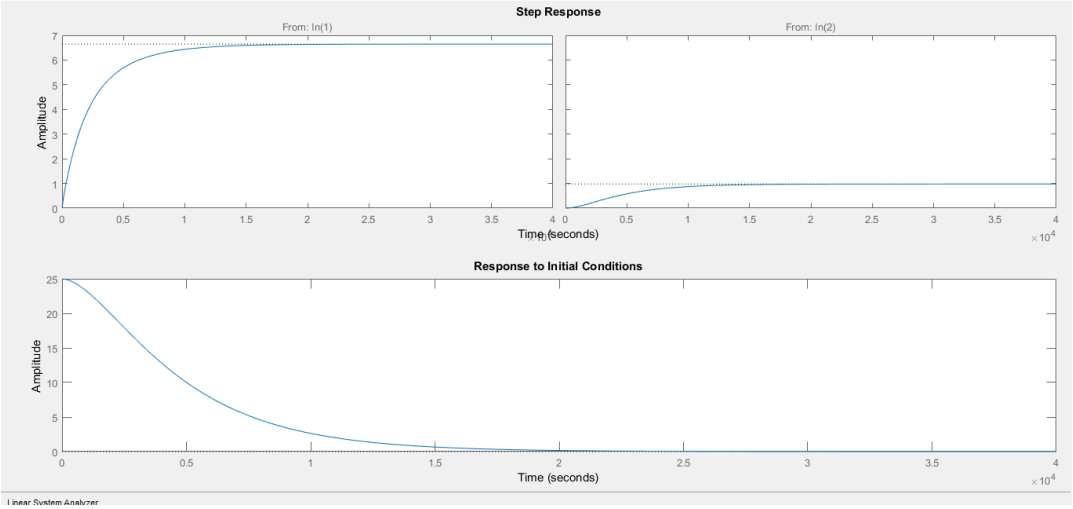

Figure 5.1: MATLAB Linear System Analysis of Temperature Model Transfer Function. The two graphs at the top represent the step response of the system from both inputs to the system: the heater wattage and the ambient temperature. At the bottom is the system's response to initial conditions.

One way to test if a system is truly first order or of a high order is by varying the DC gain. The gain margin is one way of determining by how much a system's DC gain can be changed without affecting its stability. However, for our system, it was determined that the gain margin was infinite, meaning that it would be unconditionally stable (in theory).

The *damp* function in MATLAB was used to determine the damping ratio and it was observed that the system was critically damped. However, this does not mean much as first order systems are always critically damped. Therefore, before any further analysis could be done, the system's order was to be reduced using MATLAB's *balreal* and *modred* function. The reduced system is of the third order and is seen to be almost indistinguishable from the original system (the graph from input 1).

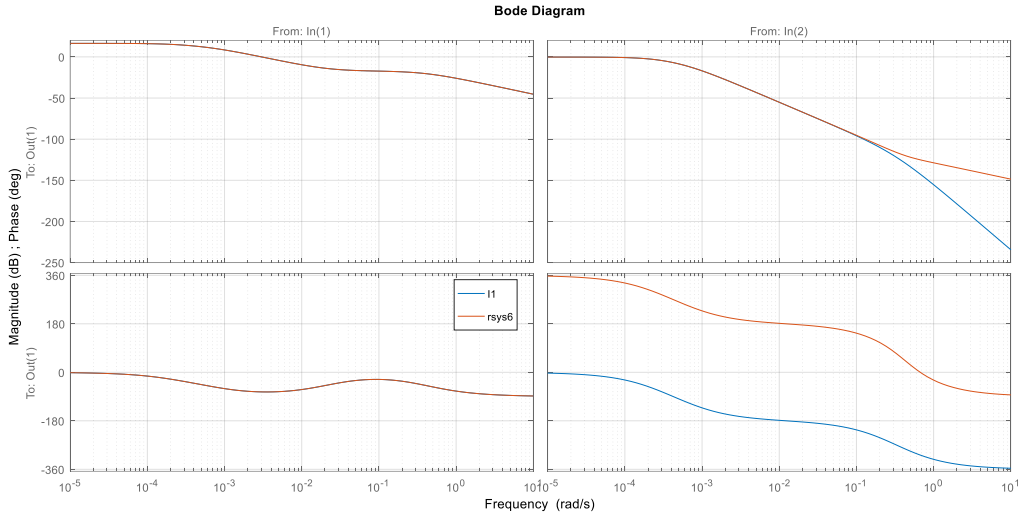

Figure 5.2: Bode diagrams (both phase and magnitude plots) of the initial fourth order system and the reduced third order system. In() represents the input to the system; input one: the heater wattage, is the model of focus for this project. The reduced transfer function of input 1 is almost indistinguishable from the original fourth order system.

The resulting transfer function is as seen in Equation 23.

rsys6 =

$$\frac{0.05415\ s^2 + 0.001216\ s + 4.697e\text{-}07}{s^3 + 0.394\ s^2 + 0.0003633\ s + 7.068e\text{-}08} \qquad (23)$$

The closed loop step response of the transfer function, $rsys6$, is as seen in Figure 5.3.

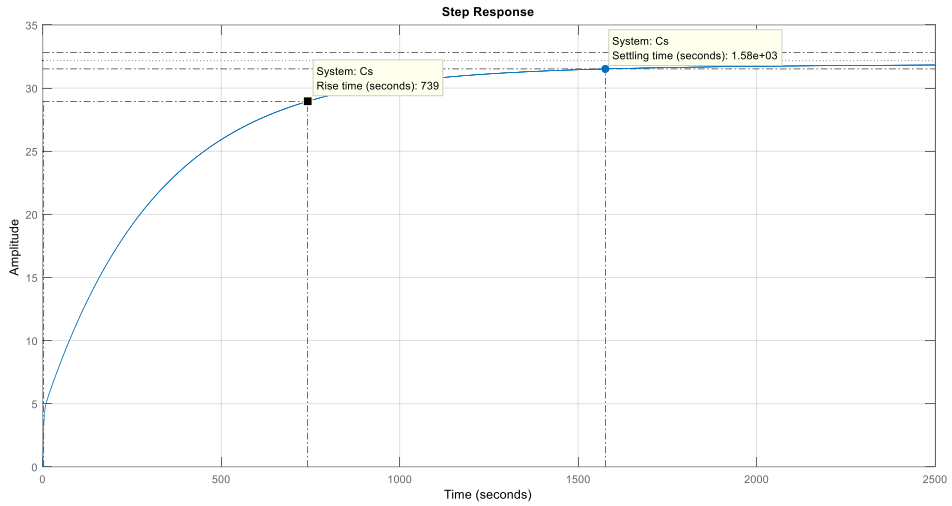

Figure 5.3: Closed loop step response of the transfer function rsys6

The rise and settling time of the system are about $12.3\,min$ and $26.3\,min$ respectively. The steady state error is 5.2481. Given that there is no overshoot whatsoever, the only characteristics that can be improved are the settling and rise times and the steady state error. Temperature is a particle property and would benefit more from derivative action. Also, from Table 4.1, it was determined that a PID controller will be best to use for this application. However, a PD and PID controller were both tested to determine which would yield the best response.

5.1.1 PD Controller

Both the PD and PID controllers were implemented using MATLAB's Control System Designer. The compensator formula for the PD controller is given by the formula in Equation 24.

$$C = 4.778 \qquad (24)$$

The step response of the system is as seen in Figure 5.4.

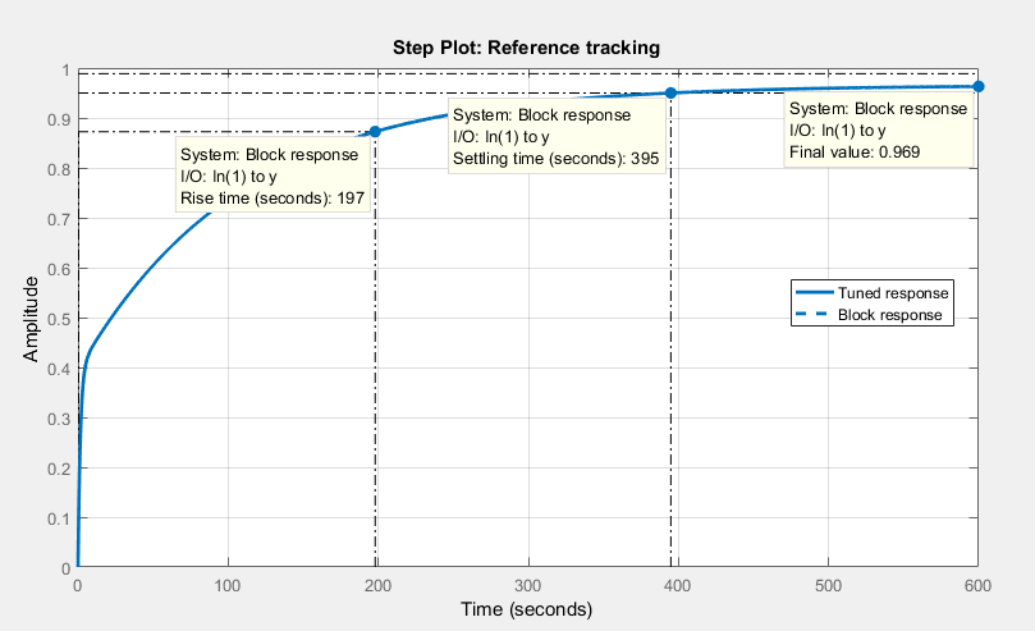

Figure 5.4: Step response of the system with a proportional and derivative controller in series with the plant transfer function

The rise time is $3.283min$, settling time is $6.583min$, percentage overshoot is approximately 0%, and steady state error is 0.031.

5.1.2 PID Controller

The compensator formula for the PID controller is given in Equation 25 and the system's step response can be observed in Figure 5.5.

$$C = 5.2022 + \frac{1.15}{s} - 2.4796\frac{2.0979}{1 + \frac{2.0979}{s}} \qquad (25)$$

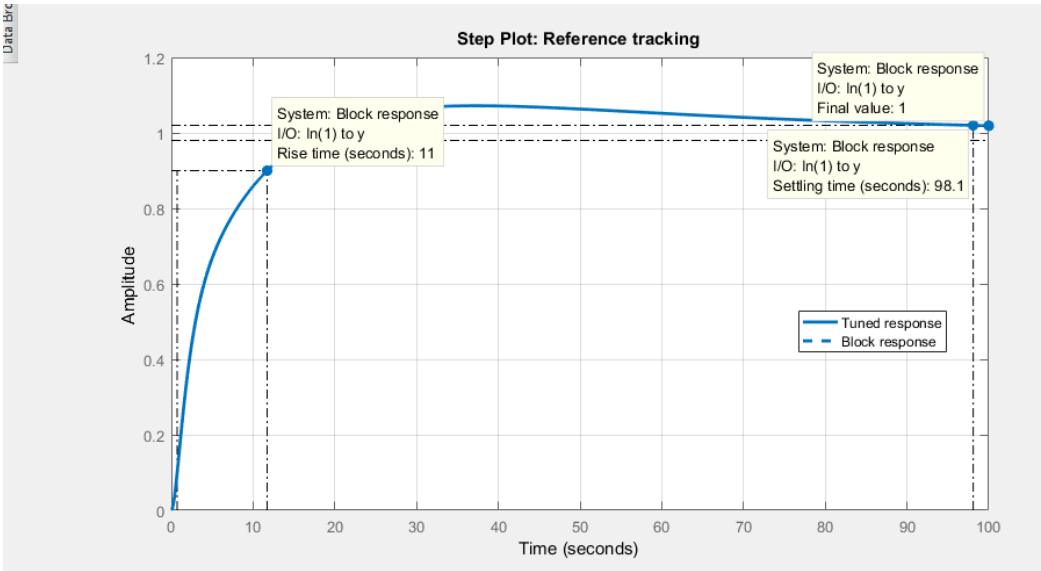

Figure 5.5: Step response of the system with a proportional, integral and derivative controller in series with the plant transfer function.

The rise time is $0.01833min$, settling time is $1.635min$, percentage overshoot is 0.6989%, and steady state error is 0.

5.2.Model Results

From Chapter 4.4.2, the model under investigation, as given in Equation 17 was solved using MATLAB's *ode45* function. The parameter, ε, was varied randomly to determine its effect on the logistic curve. The elongation rate of the length of each bacterium was also solved using MATLAB's *ode45* function. Figure 5.6 shows a graph of the length of bacteria as a function of time responding to mechanical stress. A linear curve was fitted onto the original curve to determine if the expansion rate of bacteria was linear as assumed. Figures 5.7 shows a comparison between the normal logistic curve and the tweaked version with $\varepsilon = 10$ and 100. K was chosen to be 200, $N_o = 10$, $\mu = 0.693 * \frac{10^{-3}kg}{s}$, $v = \frac{1m}{s}$, $l_o = 4 * 10^{-6}m$, $h = 0.1m$ and $r = 0.01/s$. The elongation rate of bacteria was determined by MATLAB's *ode45* function.

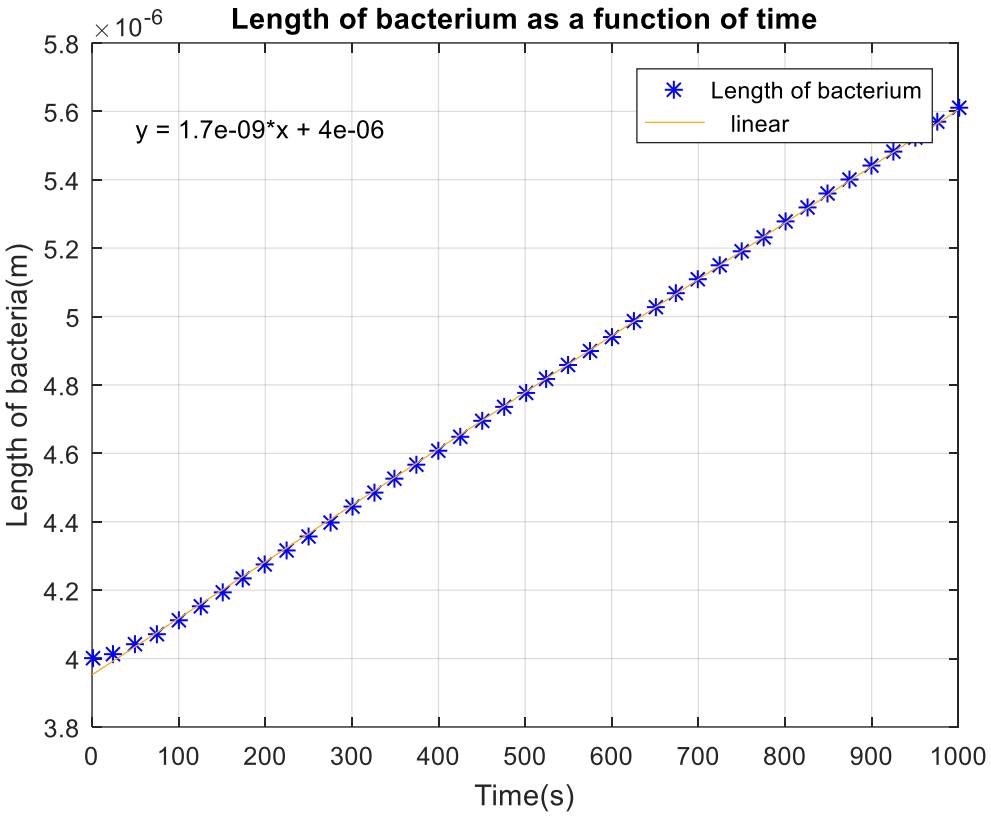

Figure 5.6: Graph of final length of bacteria as a function of time

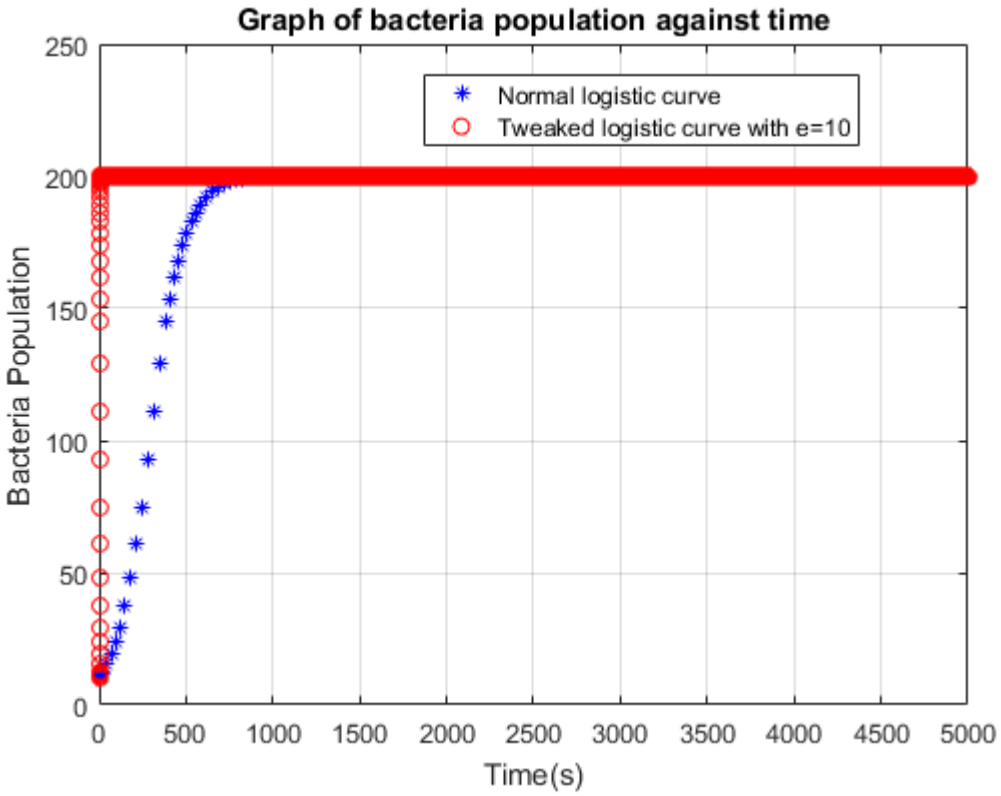

Figure 5.7: Graph of bacteria population against time for both a "normal" logistic curve and the proposed logistic curve (including the effect of shear stress on bacteria population). The varied parameter in this case was assigned a value of 10.

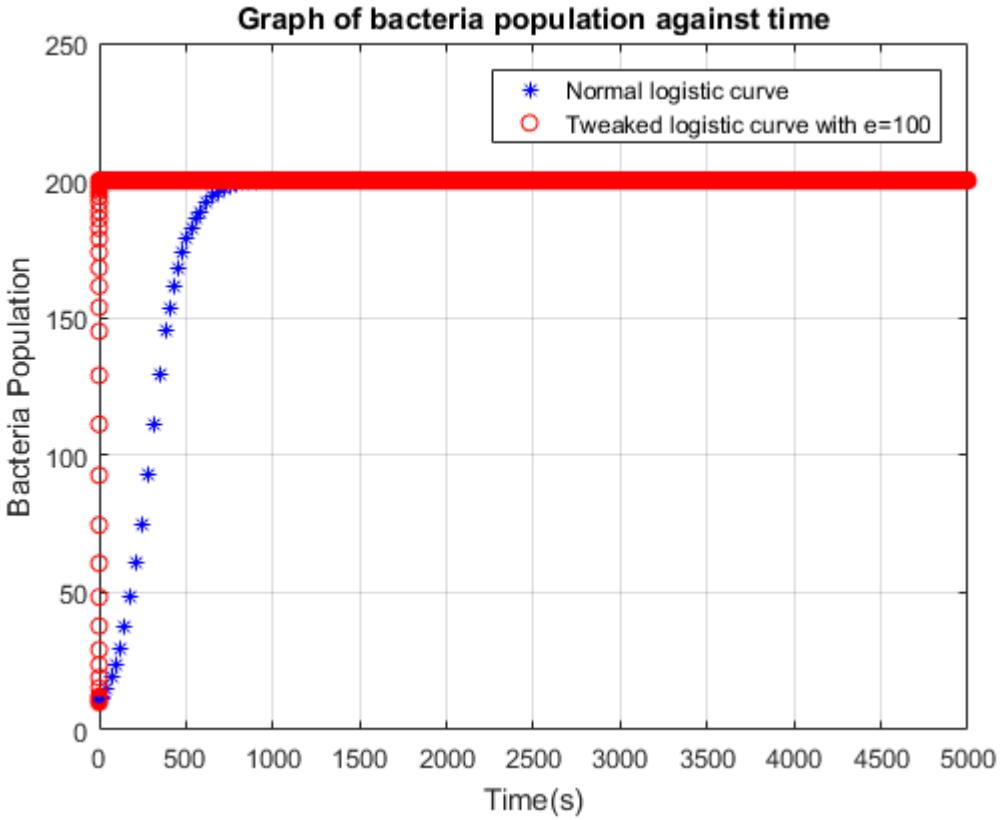

Figure 5.8: Graph of bacteria population against time for both a "normal" logistic curve and the proposed logistic curve (including the effect of shear stress on bacteria population). The varied parameter in this case was assigned a value of 100

Chapter 6: Conclusion

6.1 Discussion of Results

6.1.1 Temperature Controller

From Chapter 4.4, the system's requirements are given as follows:

- Desired tolerance: $37℃ \pm 2℃$
- Settling time $\leq 5min$
- Steady State error ≤ 0.05
- Overshoot $\leq 11\%$

From Figure 5.4, it is observed that all the system's requirements were met. However, from the compensator formula, it is noticed that the derivate action is not necessary, and the controller is purely a proportional controller.

From Figure 5.5, the PID controller appears to meet all system's requirements, just like the PD controller, but with better results. However , the PD controller will be the better pick because of its simplicity and its ease in implementation. Although the PID controller met the system's requirements better than the PD controller, it is more costly and complex to implement.

6.1.2 Mathematical Model

In Chapter 4.5, one of the assumptions of the mathematical model is for each bacterium to have a linear expansion rate. From Figure 5.6, it is observed that the fitted linear curve is almost indistinguishable from the actual curve generated and therefore, the assumption has been met.

From Figures 5.7 and 5.8, it is observed that the exponential growth phase of the modified logistic curve has been "shifted" to the left, meaning that growth occurs much

quicker than for a usual logistic model. This matches the expectations of the effect of shear stress on bacteria growth. The modified logistic curves with $\varepsilon = 10$ and 100 were also compared as seen in Figure 5.9. It is observed that there is no indistinguishable difference between the two curves, and this might be due to the exponential term introduced in the tweaked logistic mathematical equation.

6.2 Limitations

- Lack of experimental data to properly fit the tweaked logistic curve to determine the value of the parameter, ε.
- The method for calculating the inverse kinematics of the robot could not determine if the robot could move to the joint angles calculated.

6.3 Future Works

- Instead of trying to derive an analytical solution for the inverse kinematics of the robot, where it is difficult to tell if joint angles produced will result in an end-effector position outside the robot's workspace, it will be expedient to try and derive the trajectory of the robot by using the pseudo-Jacobian method instead of the Denavit-Hartenberg convention.
- Instead of reducing the system by using the Grammian based balanced system reduction from fourth order to third order, a better method of approximation would be to use particle swarm optimization.
- The model will be more accurate if the increase in the oxygen transfer rate due to the movement of the delta robot is included as a term that affects the carrying capacity of the bacterial population.
- A more credible model can be formulated by using real data and fitting it to the tweaked logistic curve to determine the value of the parameter, ε. Also, instead of assuming an

arbitrary value for the velocity of the robot, the pseudo-inverse Jacobian method used to determine the angles can also be used to determine the velocity of the robot as a function of time or, the robot can be left to run and the velocity readings from an accelerometer can be used to determine the velocity of the robot as a function of time.

6.4 Conclusion

Bacteria, specifically, *E.coli*, require more than just biological conditions to grow optimally, mechanical stimuli also affect their growth. It is therefore expedient for more researchers to delve into this area. This project provides high level understanding of the effect of mechanical stimuli in bacteria growth, provided all other known factors are kept at their optimum level and can therefore be built on to get a low level understanding to make cell culturing more than a wild shot in the dark.

References

[1] J. Ali, J. Najeeb, M. Asim Ali, M. Farhan Aslam and A. Raza, "Biosensors: Their Fundamentals, Designs, Types and Most Recent Impactful Applications: A Review", *Journal of Biosensors & Bioelectronics*, vol. 08, no. 01, pp. 1-3, 2017. Available: https://www.omicsonline.org/open-access/biosensors-their-fundamentals-designs-types-and-most-recent-impactful-applications-a-review-2155-6210-1000235.pdf. [Accessed 12 November 2018].

[2] P. Mehrotra, "Biosensors and their applications - A review", *Journal of Oral Biology and Craniofacial Research*, vol. 6, no. 2, pp. 153-159, 2016. Available: https://www.ncbi.nlm.nih.gov/pmc/articles/PMC4862100/. [Accessed 12 November 2018].

[3] French CE, de Mora K, Joshi N, et al. "Synthetic Biology and the Art of Biosensor Design". In: Institute of Medicine (US) Forum on Microbial Threats. The Science and Applications of Synthetic and Systems Biology: Workshop Summary. Washington (DC): National Academies Press (US); 2011. A5. Available from: https://www.ncbi.nlm.nih.gov/books/NBK84465/

[4] C. Cox, N. Bavi and B. Martinac, "Bacterial Mechanosensors", *Annual Review of Physiology*, vol. 80, no. 1, pp. 71-93, 2018. Available: https://www.researchgate.net/publication/321453958_Bacterial_Mechanosensors. [Accessed 4 January 2019].

[5] J. Winkle, O. Igoshin, M. Bennett, K. Josić and W. Ott, "Modeling mechanical interactions in growing populations of rod-shaped bacteria", Physical Biology, vol. 14, no. 5, p. 055001, 2017.

[6] P. Alexandre, C. Nadell, M. Kim, F. Ingremeau, A. Siryaporn, K. Drescher, N. Wingreen, B. Bassler, Z. Gitai and H. Stone, "The Mechanical World of Bacteria", Cell, vol. 161, no. 5, pp. 988-997, 2015.

[7] J. Milstein and J. Meiners, "On the role of DNA biomechanics in the regulation of gene expression", Journal of The Royal Society Interface, vol. 8, no. 65, pp. 1673-1681, 2011.

[8] P. Shapira, S. Kwon and J. Youtie, "Tracking the emergence of synthetic biology", *Scientometrics*, vol. 112, no. 3, pp. 1439-1469, 2017. Available: https://www.ncbi.nlm.nih.gov/pmc/articles/PMC5533824/. [Accessed 4 January 2019].

[9]"Addgene: Synthetic Biology - Overview", *Addgene.org*. [Online]. Available: https://www.addgene.org/synthetic-biology/. [Accessed: 05- Jan- 2019].

[10] N. Bhalla, P. Jolly, N. Formisano and P. Estrela, "Introduction to biosensors", *Essays In Biochemistry*, vol. 60, no. 1, pp. 1-8, 2016. Available: https://www.ncbi.nlm.nih.gov/pmc/articles/PMC4986445/. [Accessed 5 January 2019].

[11] R. Monošík, M. Streďanský and E. Šturdík, "Biosensors - classification, characterization and new trends", *Acta Chimica Slovaca*, vol. 5, no. 1, pp. 109-120, 2012. Available: http://www.acs.chtf.stuba.sk/papers/acs_0117.pdf.[Accessed 5 January 2018].

[12] M. Thakur and K. Ragavan, "Biosensors in food processing", *Journal of Food Science and Technology*, vol. 50, no. 4, pp. 625-641, 2012. Available: https://www.ncbi.nlm.nih.gov/pmc/articles/PMC3671056/#Sec9title. [Accessed 7 January 2018].

[13] M. Park, S. Tsai and W. Chen, "Microbial Biosensors: Engineered Microorganisms as the Sensing Machinery", *Sensors*, vol. 13, no. 5, pp. 5777-5795, 2013. Available: https://www.ncbi.nlm.nih.gov/pmc/articles/PMC3690029/. [Accessed 7 January 2019].

[14] E. Korotkaya-, "Biosensors: Design, Classification, and Applications in the Food Industry", *Foods and Raw Materials*, vol. 2, no. 2, pp. 161-171, 2014. Available: http://jfrm.ru/files/archive/4/19.pdf. [Accessed 7 January 2019].

[15] Q. Gui, T. Lawson, S. Shan, L. Yan and Y. Liu, "The Application of Whole Cell-Based Biosensors for Use in Environmental Analysis and in Medical Diagnostics", *Sensors*, vol.

17, no. 7, p. 1623, 2017. Available: https://www.ncbi.nlm.nih.gov/pmc/articles/PMC5539819/. [Accessed 7 January 2019].

[16] P. Rajkumar, T. Ramprasath and G. Selvam, “A simple whole cell microbial biosensors to monitor soil pollution”, *New pesticides and soil sensors*, vol. 10, Academic Press, 2017, pp. 437-481.

[17] R. Noor, Z. Islam, S. Munshi and F. Rahman, "Influence of Temperature on Escherichia coli Growth in Different Culture Media", *JOURNAL OF PURE AND APPLIED MICROBIOLOGY*, vol. 7, no. 2, pp. 899-904, 2013. Available: https://www.researchgate.net/publication/233761514_Influence_of_Temperature_on_Escherichia_coli_Growth_in_Different_Culture_Media. [Accessed 23 April 2019].

[18] "Shaking Incubators | VWR", *Us.vwr.com*. [Online]. Available: https://us.vwr.com/store/category/shaking-incubators/596161. [Accessed: 23- Apr- 2019].

[19] "Price Microbiology Incubator, Wholesale & Suppliers - Alibaba", *Alibaba.com*. [Online]. Available: https://www.alibaba.com/showroom/price-microbiology-incubator.html. [Accessed: 23- Apr- 2019].

[20] "Predicting Optimal Bacterial Growth", *Laboratory Equipment*, 2011. [Online]. Available: https://www.laboratoryequipment.com/article/2011/08/predicting-optimal-bacterial-growth. [Accessed: 23- Apr- 2019].

[21] A. Miller et al., "A Robust Incubator to Improve Access to Microbiological Culture in Low Resource Environments", *Journal of Medical Devices*, vol. 13, no. 1, p. 011007, 2019. Available: 10.1115/1.4042206.

[22] E. Clasen, K. Land and T. Joubert, "Micro-incubator for bacterial biosensing applications", in *Fourth Conference on Sensors, MEMS and Electro-Optic Systems*, Skukuza, 2016.

[23] H. Andersson, V. Mattsson and A. Senek, "Implementation of PID control using Arduino microcontrollers for glucose measurements and micro incubator applications", Uppsala University, 2015.

[24] "Point of Care Trends | PDT", *Pdt.com*. [Online]. Available: https://www.pdt.com/2016-point-of-care-trends.html. [Accessed: 23- Apr- 2019].

[25] [Online]. Available: http://2017.igem.org/Team:AshesiGhana#!. [Accessed: 23- Apr- 2019].

[26] A. Chamorro-Garcia and A. Merkoçi, "Nanobiosensors in diagnostics", *Nanobiomedicine*, vol. 3, p. 184954351666357, 2016. Available: https://journals.sagepub.com/doi/full/10.1177/1849543516663574. [Accessed 23 April 2019].

[27] S. Burge, *Burgehugheswalsh.co.uk*. [Online]. Available: https://www.burgehugheswalsh.co.uk/uploaded/1/documents/pugh-matrix-v1.1.pdf. [Accessed: 23- Apr- 2019].

[28] "Delta robot kinematics - Tutorials", *Forums.trossenrobotics.com*, 2009. [Online]. Available: http://forums.trossenrobotics.com/tutorials/introduction-129/delta-robot-kinematics-3276/?page=3. [Accessed: 23- Apr- 2019].

[29] "Full 3D printed DELTA robot | ChrisHerring.net", *Chrisherring.net*, 2014. [Online]. Available: http://www.chrisherring.net/all/full-3d-printed-delta-robot/. [Accessed: 23- Apr- 2019.

[30] "Coordinate Systems – ManufacturingET.org", *Manufacturinget.org*. [Online]. Available: http://www.manufacturinget.org/home/4476-computer-aided-manufacturing/fundamentals-of-g-code-programming/. [Accessed: 23- Apr- 2019].

[31] Y. Çengel and J. Cimbala, *Fundamentals of thermal-fluid sciences*, 5th ed. New York: McGraw-Hill Higher Education, 2012, p. 661.

[32] Kiam Heong Ang, G. Chong and Yun Li, "PID control system analysis, design, and technology", *IEEE Transactions on Control Systems Technology*, vol. 13, no. 4, pp. 559-576, 2005. Available: 10.1109/tcst.2005.847331.

[33] K. Todar, "Growth of Bacterial Populations", *Textbookofbacteriology.net*. [Online]. Available: http://textbookofbacteriology.net/growth_3.html. [Accessed: 23- Apr- 2019].

Appendix A: MATLAB Codes

```
%The Delta script computes the motor angles needed to position the end
%effector at a specified location (contained in the vector P). The
%DH_Transform script converts from base to motor coordinates and this is
used in
%this script.
%The parameters are:
%   P - Matrix specifying end effectors position
%   Lb - Length of the bicep
%   O - Vector containing bicep offsets from motors
%   theta - Angle between the bicep and the x-axis of the motor
coordinate frame
%Created by Nana Oye Djan
%Purpose: Capstone Inverse Kinematics
%% Function for computing the denavit hartenberg transform
function[theta] = Delta(P,O,Lb)
theta = sym('theta',[2 1]);
sym pi;
%Denavit hartenberg Transformation Matrix.
Joint1 = (DH_Transform(theta(1),0,-pi/2,0.07));
Joint2 = (DH_Transform(theta(2),0,0,Lb));
Motor =  Joint1 *translation(0, 0, -O(1)) * Rz(0);

%Final Transformation matrix for the motor
TMotor1 = (Joint2 * Motor);

%Computing the inverse of Joint1, which is A01^-1
I_1 = (inv(Motor));

%Creating the T-Variable Matrix, which is another way of representing
the
%transformation matrix. We want to multiply A01^-1 by the T-Variable
matrix
%and equate it to A12, which is Joint2.
syms n1 n2 n3 o1 o2 o3 a1 a2 a3 p1 p2 p3
n = [n1;n2;n3;0];
o = [o1;o2;o3;0];
a = [a1;a2;a3;0];
p = [P(1);P(2);P(3);1];
T_var = [n o a p];
T_var1 = I_1 * T_var;
Tvar1_4 = T_var1((1:3),4);
Joint2_4 = Joint2((1:3),4);

%Now equating A12 to A01^-1*T-variable matrix
% M = vpasolve(Tvar1_4==Joint2_4,theta);
% M.theta1
% M.theta2
S1 = vpasolve(Joint2_4(1) == Tvar1_4(1),theta);
S1.theta1;
F1 = (wrapToPi((S1.theta1)));
S1.theta2;
F2 = (wrapToPi((S1.theta2)));
S2 = vpasolve(Joint2_4(2) == Tvar1_4(2),theta);
S2.theta1;
F3 = (wrapToPi((S2.theta1)));
S2.theta2;
```

```
F4 = (wrapToPi((S2.theta2)));
S3 = vpasolve(Joint2_4(3) == Tvar1_4(3),theta);
theta1 = [F1;F3];
theta2 = [F2;F4];
theta = [theta1 theta2];
end



%This script basically plots the state space model data from Simulink,
determines and reduces the transfer function from the Simulink data and
%reads temperature data from Arduino, and tunes it using the Kp and Kd
values.
%Created by Nana Oye Djan
%Purpose: Capstone Temperature Control
%% Plotting results from Simulink Model
figure
plot(Incubator_Temperature)
grid on
title('Determining the order of the thermal dynamics of the incubator')
ylabel('Temperature(oC)')
xlabel('Time(s)')
axis([0 80000 0 300])
%% Determining the transfer function
A = [-0.37155 0.371552 0 0;0.0215 -0.02206 0.000548697 0;0 0.000056022 -
0.0007496 0.0006936;0 0 0.14079 -0.275466];
B = [0.05415 0;0 0;0 0;0 0.13467];
C = [1 0 0 0];
D = [0 0];
I1 = ss(A,B,C,D);
[num1,den1] = ss2tf(A,B,C,D,1);
sys1 = tf(num1,den1);
[rsys,sigma1,Ti,Td] = balreal(I1);
rsys6 = modred(rsys,3:4,'Truncate');
sys2 = tf([1],[1]);
CLR = feedback(rsys6,sys2);
%% Temperature read functions (for the DHT11 sensor)
delete(instrfind)
% a = arduino('COM8');
s = serial('COM8');
fopen(s);
current_output = fscanf(s,'%d');
desired_temp = 37;
error = current_output - desired_temp;
prev_error = 0;
error_change = error - prev_error;
Kp = 4.778;
Kd = 0;
%% Acquiring live data and Implementing P controller
figure
h = animatedline;
Axis = gca;
Axis.YGrid = 'on';
Axis.YLim = [15 50];
stop = false;
startTime = datetime('now');
while ~stop;
    % Correct temperature using PD controller
    TR = (Kp*error)+(Kd*error_change);
    heater = writeAnalogPin(a,'A3');
    current_output = fscanf(s,'%f');
```

```
    prev_error = error;
    error = current_output - desired_temp;
    error_change = error - prev_error;
    % Get current time
    t =  datetime('now') - startTime;
    % Add points to animation
    addpoints(h,datenum(t),current_output)
    % Update axes
    ax.XLim = datenum([t-seconds(15) t]);
    datetick('x','keeplimits')
    drawnow
    grid on
    xlabel('Elapsed time');
    ylabel('Temperature(degrees Celsius)');
    legend('Temperature','Adjusted temperature')
    stop = readDigitalPin(a,'D7'); %A push button will be used to stop
the
    %incubator
end
%% Plotting the recorded data
[timeLogs,tempLogs] = getpoints(h);
timeSecs = (timeLogs-timeLogs(1))*24*3600;
figure
plot(timeSecs,tempLogs)
xlabel('Elapsed time')
ylabel('Temperature(degrees Celsius)')
grid on
legend('Adjusted Temperature')
%% Saving the data
T =
table(timeSecs',tempLogs','VariableNames',{'Time_sec','Read_Temp_C'});
filename = 'C:\Users\hp\OneDrive - Ashesi University\Nana Oye Djan -
Ashesi\Spring 2019\Senior Project\Temperature
Control\Temperature_Data.xlsx';
% Write table to file
writetable(T,filename);
```

```
%This script computes the tweaked logistic curve differential equation
%Created by Nana Oye Djan
%Purpose: Capstone Tweaked Logistic Curve Equation
function Nprime1 = Delta_log_growth(t1,N1,Lfinal)
K = 200;
rmax = 0.01;
viscosity = 0.693*10^-3;
velocity = 1;
height = 0.08;
shear_rate = velocity / height;
tau = viscosity * shear_rate;
value = 1;
e_rate = 1.7*10^-9;
erate = e_rate./Lfinal;
er = mode(erate);
Nprime1 = ((rmax.*N1)*(1-(N1/K))).*((exp(tau)./(rmax.*er.*value)));
%Nprime1 = ((rmax*N1)*(1-(N1/K)))*(((tau)./(rmax*erate*value)));
end

%This script computes the elongation rate of bacteria with the
assumption
%that it is linear
```

```
%Created by Nana Oye Djan
%Purpose: Capstone Cell Elongation Rate
function elongation_rate = Cell_expansion_rate(t2,Lfinal)
alpha = 1.6667*10^-9;
y = 0.693*10^-3;
k = 1*10^-5;
const = y/(2*k);
Lo = 4*10^-6;
Lt = 2*Lo;
if Lfinal<Lt
    elongation_rate = (alpha*(1-(exp(-t2/const))));
else
    elongation_rate = 0;
end
end
```

```
%This script computes the logistic curve differential equation
%Created by Nana Oye Djan
%Purpose: Capstone Logistic Equation Curve
function Nprime = log_growth(t,N)
K = 200;
rmax = 0.01;
Nprime = (rmax*N)*(1-(N/K));
end
```

```
%This script solves the differential equation from the Cell expansion
rate
%script.
%Created by Nana Oye Djan
%Purpose: Capstone Elongation rate
Tspan = [0 5000];
Lo = 4*10^-6;
[t2,Lfinal] = ode45('Cell_expansion_rate', Tspan, Lo);
plot(t2,Lfinal,'b*')
grid on
```

```
%This script solves the differential equation from the log growth and
Delta
%log growth rate scripts.
%Created by Nana Oye Djan
%Purpose: Capstone Growth rate
Tspan = [0 5000];
No = 10;
[t,N] = ode45('log_growth', Tspan, No);
Lo = 4*10^-6;
[t1,N1] = ode45(@(t1,N1) Delta_log_growth(t1,N1,Lfinal),Tspan,No);
[t2,Lfinal] = ode45('Cell_expansion_rate',Tspan,Lo);
plot(t,N,'b*')
grid on
hold on
plot(t1,N1,'ro')
```